VOL. 16 No. 12, pp. 341-372 JUNE 1955

Philips Technical Review

DEALING WITH TECHNICAL PROBLEMS
RELATING TO THE PRODUCTS, PROCESSES AND INVESTIGATIONS OF
THE PHILIPS INDUSTRIES

EDITED BY THE RESEARCH LABORATORY OF N.V. PHILIPS' GLOEILAMPENFABRIEKEN, EINDHOVEN, NETHERLANDS

FOREIGN ATOMS IN METALS

by J. D. FAST.

669.017

For many readers, the title of this article will perhaps already evoke the many publications by the same author, both in this journal and elsewhere. The cross-section of his field of study considered here by Prof. Fast — viz. interstitial solutions — formed the principal contents of his inaugural lecture on his appointment as extra-mural professor at Delft on 12th January 1955. The lecture is supplemented here by illustrations and references to the literature.

It is perhaps not always fully realized how important is the role of metals in our lives. Modern civilization would be out of the question without the generation and distribution of electrical energy, without the production and distribution of town-gas and drinking-water, without motor traffic, trains, ships and aircraft, without printing and communications, the telegraph, telephone, radio, television and the film. Our civilization could not exist without surgery, without large industries employing all manner of machines, apparatus and measuring instruments, without bridges, cranes and docks, without electric lighting, vacuum cleaners and typewriters. If there were no metals at our disposal, none of these could have been developed to their present advanced state. Metals played an important role even in primitive communities, especially for making weapons, tools, jewellery and coinage. Indeed, the vital role of certain metals is illustrated by the fact that the history of mankind distinguishes a copper age, a bronze age and an iron age.

Of the hundred or so elements more than two-thirds are metals. In ancient times only seven of these metals were known: copper, silver, gold, mercury, tin, lead and iron. By about 1900 many more were known, but only five of the newcomers have found their way into the ranks of the metals of industrial importance: magnesium, zinc, aluminium, antimony and nickel. Aluminium, the most important of the five, can be produced economically on a large scale only by electrolytic methods; it thus had to wait for the birth of electrical technology in the latter half of the last century.

It remained for the present century to see the application of the mass of the metallic elements. Besides the dozen metals which have been named, the following metals are among those which are now used industrially on a considerable scale: sodium, caesium, beryllium, calcium, barium, cadmium, indium, titanium, zirconium, thorium, germanium, vanadium, niobium, tantalum, chromium, molybdenum, tungsten, uranium, manganese and cobalt. The availability of all these metallic elements has led to the development of a vast number of useful alloys; a survey of the latter is quite impracticable. The metallurgist has developed all these metals in order to meet the demands of an ever-expanding technology: higher melting points, greater mechanical strength, special electrical resistance characteristics, special magnetic properties, improved corrosion resistance, etc.

Hand in hand with and as a necessary condition for this great expansion, metallurgy has developed from purely empirical techniques to an exact science: originally it comprised only extraction metallurgy (the preparation of metals from their ores), the working of metals by casting and mechanical deformation, heat treatments and mechanical testing. Metallography, the microscopic study of the structure of metals, was added in the last century.

Round about the turn of the century, a considerable advance was made when Bakhuis Roozeboom, whose centenary has been recently celebrated, demonstrated how Gibbs' phase rule may be applied to alloys. Van Laar carried this application of thermodynamics to metallurgy a stage further, by showing that the simplest types of binary phase diagrams can be completely derived from the heats of mixing and entropies of mixing for the liquid and solid states and the heats of fusion of the two components. Van Laar's important work, however, remained for ten years almost unnoticed. After 1912 the metallurgist learnt to think in terms of atoms from the pioneer work of Von Laue and the two Braggs. These investigators demonstrated with the aid of X-rays, that all crystals, and hence also the crystals from which metals are built up, are orderly, periodic configurations of atoms; further, they showed that the distances between the atoms in these configurations may be quantitatively determined. Structural investigations by means of X-ray diffraction have been continued in many laboratories, throwing new light on phase diagrams.

Initially it was expected that it would be possible to explain all the properties of a crystalline material from the structure determined from diffraction patterns. It was thought that local deviations from the perfect lattice structure would have only a slight influence on the properties. Gradually, however, it has come to be realised that many of the most interesting properties of crystals owe their origin to just these deviations from the perfect atomic configurations. This applies, for example, to the plastic deformation of metals which, according to modern theory, is due to linear imperfections in the lattice, known as dislocations. Mass transfer (diffusion) in solid metals also seems to be due to the presence of imperfections in the lattice. Point imperfections are responsible for this phenomenon, i.e. extra atoms squeezed into the orderly configuration or absent atoms (vacancies) at points where they are normally present.

Apart from the development of new metals and alloys, the metallurgist's tasks include learning to control these lattice imperfections and to employ them usefully for the improvement of the properties of the metals. A number of phenomena will now be discussed, which depend upon one type of imperfection, viz. the presence of extra atoms (interstitials) in the periodic lattice.

Examples of interstitial solutions

A metal in equilibrium can take up foreign atoms in its interstices only when the foreign atoms are relatively small. This is especially the case where the foreign atoms are certain non-metallic elements of low atomic number: hydrogen, boron, carbon, nitrogen and oxygen. The latter two elements have played a striking part in the history of the metals titanium and zirconium. All ingots made from these metals some thirty years ago were found to be brittle, even those ingots, which had been shown by chemical analysis to be very pure. Consequently it was long assumed that brittleness was an intrinsic property of titanium and zirconium. However, in 1924 a method was discovered in Eindhoven for preparing these metals in a highly ductile form [1]). The ductile metal appeared to have the same crystal structure as the brittle form, so that it had to be assumed that the latter contained one or more impurities which had not been detected by normal chemical analysis. Extensive investigation into this matter showed that titanium and zirconium could contain a considerable atomic percentage of oxygen in solid solution, and that even a few percent were sufficient to render either metal hard and brittle [2]). Nitrogen also appeared to be highly soluble in both metals and to have in the dissolved state an even more unfavourable influence on the mechanical properties than oxygen. Both non-metals are absorbed in atomic form in the largest interstices (octahedral spaces) of the hexagonal metal lattice. In the titanium and zirconium ingots prepared by the early methods it was especially oxygen which was present in an undesirably high amount. Now that this action of oxygen and nitrogen is known, it is possible in principle to add them in controlled quantities to titanium and zirconium to render the latter suitable for applications for which the pure metals are too soft. The amounts of oxygen or nitrogen must either be chosen so small that the ductility of the metal is not completely lost, or the hardening must be confined to the surface layers.

Other metals are likewise rendered hard and brittle by interstitially dissolved atoms. Hardening by means of interstitial atoms has been unknowingly employed for many centuries in the hardening of steel. In this case the hardening element is carbon. In the hardening process this element is dissolved to form a highly supersaturated solution, making use of the fact that its solubility in the iron phase stable above 900 °C (γ iron) is far greater than its solubility in the phase stable below this temperature (α iron).

---

[1]) J. H. de Boer and J. D. Fast, Z. anorg. allg. chem. **153**, 1-8, 1926.

[2]) J. H. de Boer and J. D. Fast, Rec. Trav. chim. Pays-Bas **55**, 459-467, 1936; J. D. Fast, Metallwirtschaft **17**, 641-644, 1938.

Titanium and zirconium have crystallographic transition points at about the same temperature as iron, but the technique used in the hardening of steel may not be employed here since oxygen and nitrogen dissolve far more readily in the Ti and Zr phases stable at low temperatures than in those stable at high temperatures. The same is true for carbon which, however, has a lower solubility in both metals than either oxygen or nitrogen.

This inverse effect of the crystallographic transition on interstitial solubility is illustrated by the binary phase diagrams for Fe-C, Fe-N compared with those of Ti-O, Ti-N, ... etc: the presence of interstitial atoms shifts the crystallographic

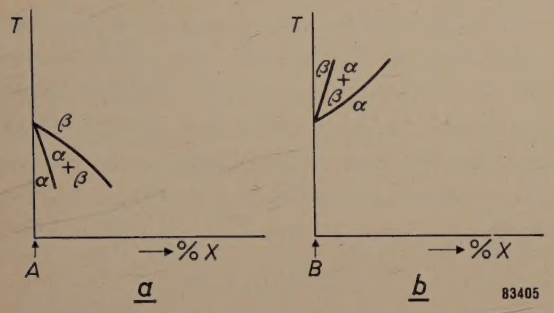

Fig. 1. *a*) The melting point or a crystallographic transition point of a component (*A*) moves to lower temperatures by adding a certain component (*X*), since the solubility in phase α stable at low temperatures is less than the solubility in phase β stable at high temperatures.
b) In the reverse case (*B*-*X* system) the melting point or or transition point is shifted to higher temperatures.

transition for iron to lower temperatures whilst that for titanium and zirconium moves to higher temperatures. This is schematically represented in *fig. 1*. *Figures 2* and *3* show larger parts of the phase diagrams for two of the binary systems discussed, viz. the Fe-C and Zr-O systems.

Factors determining the interstitial solubility

The facts mentioned above seem to indicate a connection between the size of the available interstices and the solubility of carbon, oxygen and nitrogen. The crystal structure as determined by X-ray diffraction, shows that the γ phase of iron has larger interstices than the α phase, and it can indeed dissolve more carbon and nitrogen; in the case of Ti and Zr however it is the phases stable at lower temperatures which have the larger interstices and which can dissolve the greater quantities of C, N and O. The introduction of a carbon, nitrogen or oxygen atom into an interstice of a metal involves an appreciable local strain in the lattice. The smaller the size of the interstice relative to the interstitial atom, the more will the lattice be deformed and the greater will be the deformation energy, required

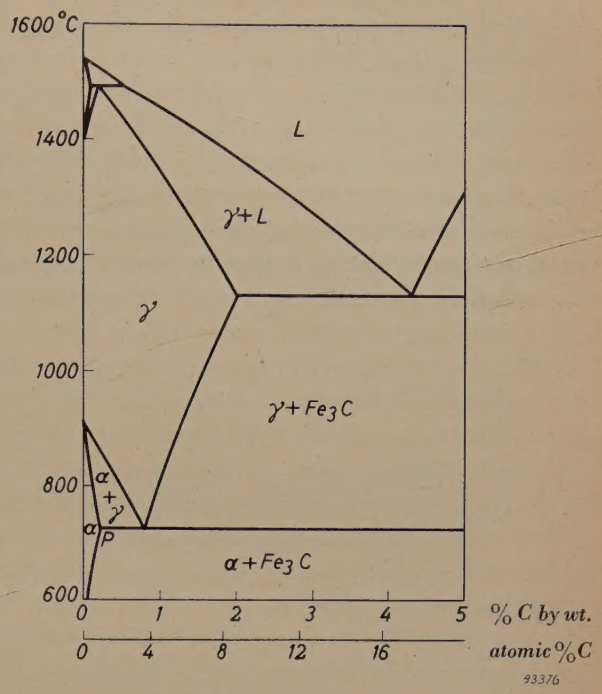

Fig. 2. A part of the iron-carbon phase diagram. For the sake of clarity the distance of *P* from the % $C = 0$ axis has been exaggerated; in reality the maximum solubility of carbon in α iron corresponding to this point is only 0.02 % by weight. *L* is the liquid phase. In contrast to fig. 1, the iron phase stable at high temperatures (above 900 °C) is designated γ iron and not β iron; this has arisen historically, since earlier it was incorrectly thought that the transition of iron at about 760 °C from the ferromagnetic to the paramagnetic state corresponded to a transition into another phase which was designated at the time the β phase.

to place it there. This greater deformation energy will mean a smaller solubility of the interstitial atoms.

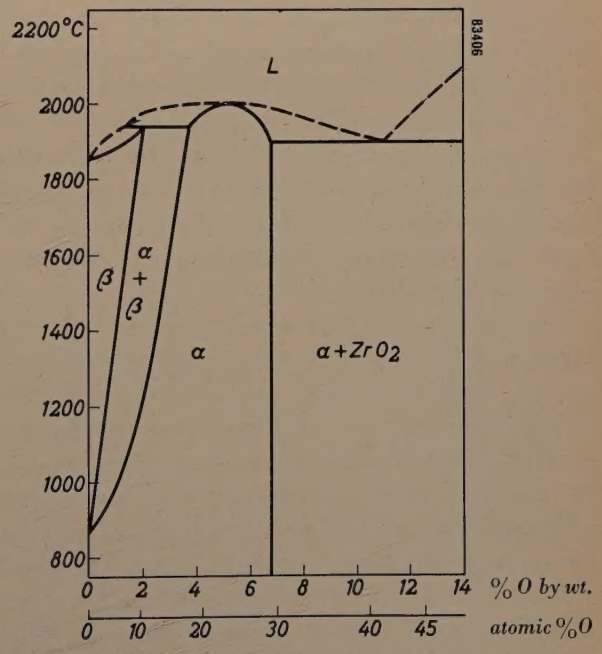

Fig. 3. A part of the phase diagram for zirconium-oxygen (From Domagala and McPherson, J. Metals **6**, 238-246, 1954).

There is a temptation to generalize the foregoing by supposing that there is a general relation between the interstitial solubility of foreign atoms and the ratio of the size of the latter to that of the interstices. Closer consideration shows that the supposition that the solubilities are determined exclusively by geometrical factors does not correspond with the facts. Even if we ignore the fact that entropy changes during solution also play a part in determining the solubility, we must nevertheless take into account the existence of two other factors besides the elastic deformation energy: the electronic interaction energy and the stability of the coexistent phase — the source of the interstitial atoms. Let us now briefly examine these two additional factors.

The significance of the electronic interaction energy is shown, for example, by the fact that helium atoms, which are smaller than either carbon or nitrogen atoms but have a highly stable configuration of two paired electrons, do not dissolve in any metal. That the interstitial atoms must be relatively small is thus a necessary but by no means sufficient condition. The heat of solution can be expressed, to a rough approximation, as the sum of the elastic deformation energy, which is always positive (absorption of heat during isothermal solution) and the electronic interaction energy, which can be either positive or negative. Strictly speaking, this division of the energy of solution into two terms is not justifiable, since the interaction energy depends to a large extent upon the interatomic distances and hence upon the deformation energy. Such a division however, is useful for many considerations. For the sake of brevity we will denote the two terms strain energy and chemical energy. A typical example of those cases in which the chemical energy is dominant is the solubility of oxygen in copper, silver and gold. In silver and gold the interstices are larger than those in copper, yet the solubility of oxygen in these metals at a given pressure decreases in the order Cu, Ag, Au, corresponding to their decreasing affinities for oxygen [3]).

The influence of the stability of the coexistent phase is illustrated by a comparison of the solubilities of carbon, nitrogen, and oxygen in iron. Although the size of the C, N and O atoms decreases in that order, the solubility of oxygen in both modifications of iron, when FeO is the second phase, is appreciably less than that of nitrogen and carbon, when Fe_4N and Fe_3C respectively are the second phases. This is no doubt largely due to the greater stability of the oxides of iron compared to the nitrides and carbides.

[3]) J. L. Meijering, Acta Metallurgica, in the press.

The strain energy

A striking picture of the important influence of the strain energy may be obtained from a study of the effects of carbon and nitrogen in iron. From purely geometrical considerations, it is possible to see a connection between many of the phenomena occurring in ordinary mild steel, which at first sight appear to have little or nothing in common. One of these phenomena, viz. the greater solubility of carbon and nitrogen in γ iron, as compared with their solubilities in α iron, has already been mentioned. The influence of the strain energy also manifests itself in each deformation of the lattice, which enlarges some of the interstices, while diminishing others. Such a deformation leads to a change in the distribution of the dissolved C or N atoms, such that the occupation of the contracted interstices decreases and that of the enlarged interstices increases. The fall in the entropy, which accompanies this departure from the random distribution, is overcompensated by a simultaneous fall in the energy, so that a net fall in free energy results from the redistribution.

Deformation by internal stresses

Deformation of the lattice, leading to redistribution, can be caused by internal as well as by external stresses. A familiar source of internal stresses are dislocations, the linear lattice defects already mentioned; these are responsible for the ready plastic deformation of metals. On one side of the slip plane of an edge dislocation, the iron lattice is stretched and on the other side of the slip plane it is compressed (see *fig. 4*). The deformation rapidly decreases as the distance from the dislocation increases. The introduction of a C or N atom into an enlarged interstice of the stretched zone will require

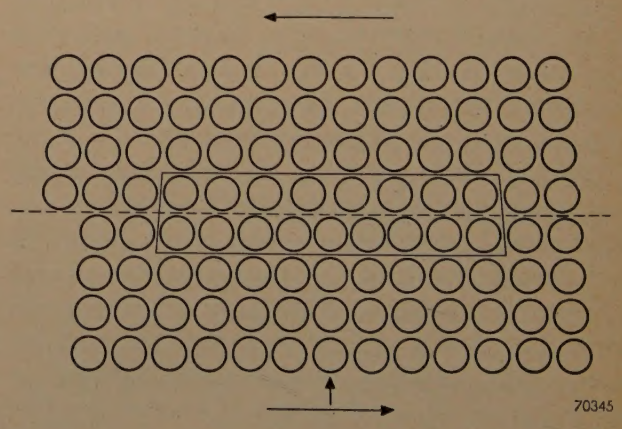

Fig. 4. Schematic respresentation of an edge dislocation in a simple cubic metal lattice. The dislocation is a linear imperfection in the lattice in a direction perpendicular to the plane of the diagram. Its effect on one atomic layer is shown here (see the enclosed region). The dotted line represents the plane in which slip can occur.

less deformation energy than introduction into a normal interstice. Dissolved C or N atoms which arrive at the dilated region by diffusion will be no longer able to leave this zone at low temperatures, e.g. room-temperature. When there are enough carbon or nitrogen atoms present in the lattice, chains of interstitial atoms will be formed along the whole length of each edge dislocation. Formation of these chains or strands greatly influences the plastic properties at ordinary temperatures, since plastic deformation (as, for example, in the tensile test)

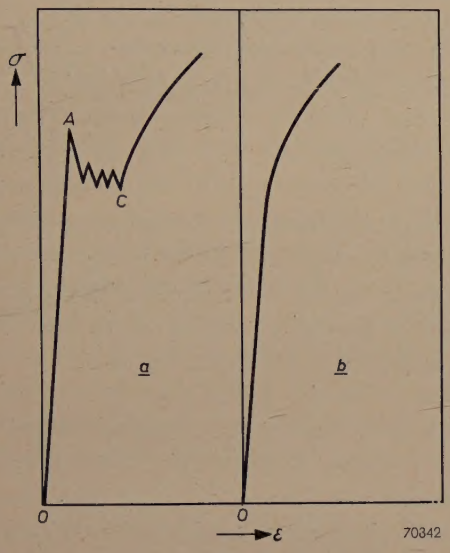

Fig. 5. Stress-strain curve for mild steel. The tensile stress σ is plotted as a function of the elongation ε.
The steel shows a sharp upper yield point at A (fig. 5*a*). If it is plastically stretched to C and the stress removed, then on renewed loading the material shows a stress-strain curve (*b*) without a yield point.

must be preceded by a freeing of the dislocations from the atom strands. This separation brings the metal into a higher energy state, the dissolved atoms being located, after the separation, in normal interstices. An extra stress is therefore initially required to move the dislocations, but after the C or N atom strands have been freed, this stress is no longer needed. This explains the occurrence of an upper and a lower yield point in the stress-strain curve for mild steel (*fig. 5*). Directly after a small plastic deformation the dislocations are still free; a well-defined yield point is lacking on renewed deformation (fig. 5*b*). If the metal is then allowed to stand, the carbon and nitrogen atoms once more diffuse towards the dislocations, as a consequence of which the upper and lower yield points are restored and the metal becomes more difficult to deform (harder). This spontaneous process has been given the name of strain ageing. The theory of the occurrence of an upper and a lower yield point and of strain ageing was originated by the English worker A. H. Cottrell [4]).

Experiments in Eindhoven [5]) have shown that strain ageing can also occur even if the C or N are not dissolved in the iron but present merely in the form of small crystals of Fe_3C or Fe_4N. Under suitable conditions, the C or N atoms move from these crystals into the iron lattice where they may reach the dislocations by diffusion. The experiments show that the C or N atoms are more strongly bound in dislocations than in the Fe_3C or Fe_4N crystals. This is the more remarkable since — as is well known — they are less strongly bound in normal interstices than in Fe_3C or Fe_4N crystals. These facts clearly show the importance of the strain energy. If the carbon or nitrogen is present in the steel only in the form of a very stable carbide or nitride (e.g. TiC or TiN) where it is bound more strongly than in a dislocation, then no strain ageing occurs.

Deformation by applied stresses

Applied stresses can also lead to a redistribution of the interstitial atoms in α-iron. This phenomenon is connected with the asymmetry of the interstices. The dissolved atoms are sited in the octahedral interstices in the iron lattice, whose centres coincide with the middle points of the edges and faces of the unit cell. The six atoms which enclose the octahedral interstice in α-iron form an irregular octahedron (one body diagonal shorter than the other two, see *fig. 6*). A carbon or nitrogen atom in such an

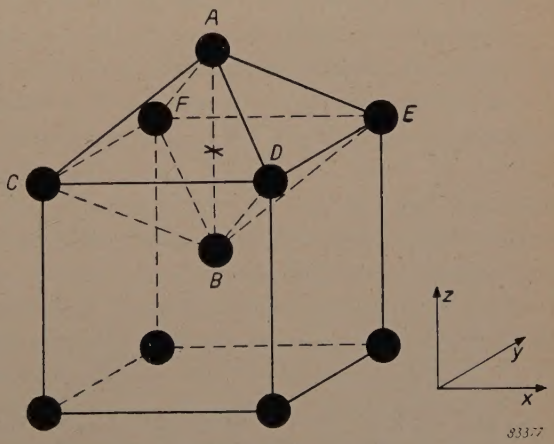

Fig. 6. The cross in the diagram indicates the location of the centre of an octahedral interstice in the unit cell of a body-centred cubic metal. Such interstices are not symmetrical with respect to the x, y and z direction: the distances CE and DF are $\sqrt{2}$ times greater than the distance AB.

[4]) A. H. Cottrell, Progress in Metal Physics **1**, 77-126, 1949.
[5]) J. D. Fast, Revue de Métallurgie **47**, 779-786, 1950; Philips tech. Rev. **14**, 60-67, 1952/53.

interstice therefore exerts a greater force on two of the six iron atoms and causes a unilateral elongation in the direction of the axis defined by these two atoms. Denoting the axes of the unit cell x, y and z, the interstices can be divided into three groups: x, y and z interstices. In an undeformed crystal, the interstitial atoms are distributed equally over the three types of interstices. This does not mean that they occupy fixed positions; the average duration of stay in any one interstice is only about a second at room-temperature. If now the crystal is stretched elastically in the direction of the x axis, there will be a preference for the enlarged x positions and a shift in the distribution equilibrium, so that the occupation of the x positions increases while that of the y and z positions decreases. This redistribution takes a certain time and leads to an extra elongation which occurs after the momentary elastic elongation and gradually reaches a limiting value (*fig. 7*). The rate at which this occurs is determined by the rate of diffusion of the dissolved C and N atoms, i.e. by the above-mentioned frequency of movement between sites — about 1 per second at room-temperature. This phenomenon is known as elastic after-effect. With an alternating load, this leads to a phase shift between load and deformation and thus to a dissipation of elastic energy, i.e. to damping of free vibrations (*fig. 8*).

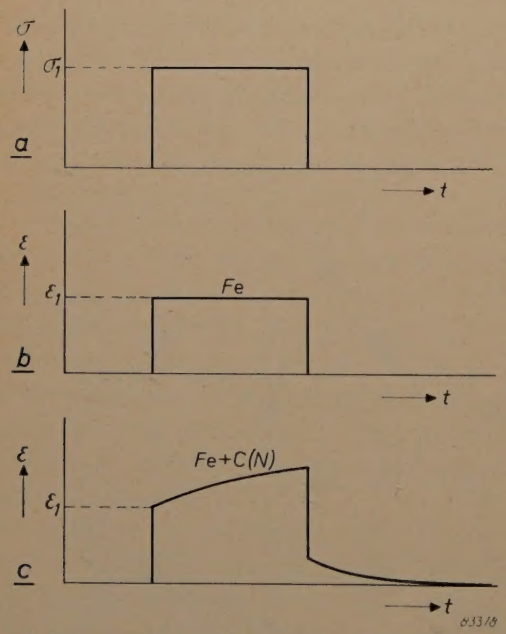

Fig. 7. *a*) A constant tensile stress σ_1 (which is considerably below the yield point) is applied at a certain instant to an iron crystal in the direction of one of the axes of the cube. *b*) The metal responds at once, showing a certain elastic elongation ε_1, which in the case of pure iron remains constant. *c*) If the iron contains dissolved carbon or nitrogen, the sudden elongation ε_1 is followed by a much smaller elongation which tends gradually to a limiting value (elastic after-effect). If at a later moment the tensile stress be suddenly removed, then in the case of pure iron the total strain disappears equally suddenly; with C or N-containing iron the same sudden shortening occurs and is followed by the gradual disappearance of the extra strain.

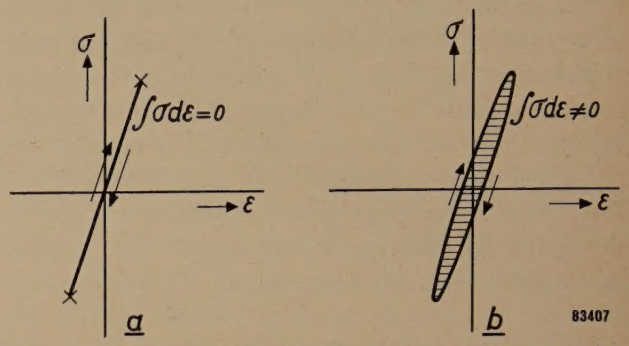

Fig. 8. *a*) For periodic loading (below the yield point) of a body which does not show the after-effect, no dissipation of vibration energy occurs. *b*) If, on the other hand, the material shows the after-effect, then the deformation ε passes its zero value later than the stress σ and energy is dissipated. The area of the shaded envelope gives the energy dissipation per cycle.

The above explanation of the elastic after-effect and damping caused by interstitial atoms was given at Eindhoven by Snoek [6]). Measurements of Snoek-damping has developed within recent years into an important aid to fundamental research on iron and steel. It has made it possible to determine with a high degree of accuracy the diffusion coefficient and solubility of carbon and nitrogen in α-iron at various temperatures. It serves also for the analytical determination of small quantities of C and N in iron and for measuring the rate at which they precipitate from supersaturated solution in α-iron. In connection with the latter it is to be noted that the solubility of carbon and nitrogen in α-iron at the temperatures of the damping measurements (in the neighbourhood of room temperature) is virtually zero, so that the measurements are performed on supersaturated solutions, obtained by rapid cooling from a higher temperature (say 500 °C). The degree of damping decreases slowly with time at, for example, 20 °C and the rate at which this decrease occurs is a direct measure of the rate of precipitation, i.e. of the rate at which carbide and nitride crystallize out in the mass of the α-iron.

Magnetostrictive deformation

No account has been taken in the foregoing of the magnetostrictive deformation of the iron lattice occurring below the Curie-point. Below the Curie-temperature iron, even in a macroscopically non-magnetic state, is always locally magnetized to saturation. If no external magnetic effect is apparent this merely indicates that the spontaneous magnetization in the various domains, the Weiss domains, is

[6]) J. L. Snoek, Physica **8**, 711-733, 1941 and **9**, 862-863, 1942.

in different directions. The directions always coincide in stress-free iron with one of the six directions of the edges of the unit cell. The iron lattice is slightly elongated in the direction of the spontaneous magnetization (magnetostriction). Hence the assertion made above that the dissolved C and N atoms in stress-free iron are equally distributed among the x, y and z positions, is true only when averaged over a large number of Weiss-domains. It does not hold for the individual domains. If the magnetization vector of a particular Weiss domain is directed, say, in the $\pm$ x-direction, there will be a pronounced preference for the x positions.

It is to be expected that the presence of dissolved C and N atoms will have a considerable influence upon the mobility of 90° domain walls (planes between Weiss-domains of mutually perpendicular magnetizations). The displacement of such a 90° domain wall corresponds to a rotation of the magnetization direction through 90° in the region covered and to a contraction of the preferential interstices in which (for the greater part) the foreign atoms are situated (*fig. 9*). This causes a rise in energy. The displacement of a 90° wall in iron containing dissolved C or N, will thus require a greater force than would be necessary for such a displacement in pure iron. It is reasonable to assume that the freedom of movement of 180° domains walls is much less influenced by the presence of dissolved C or N since the magnetostrictive deformation is not altered by the displacement of a 180° wall.

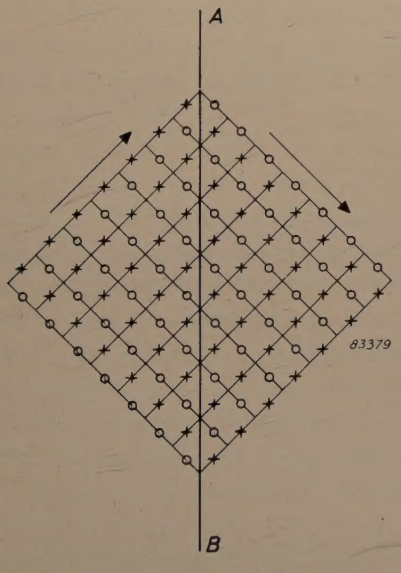

Fig. 9. The line AB represents a 90° domain wall in α-iron. The iron atoms are considered as being located at the corner points of the network. The arrows give the directions of spontaneous magnetization. To the left of AB the locations of the preferred sites for the interstitial atoms are represented by the crosses and to the right of AB by the circles. The difference of location is a consequence of the small magnetostrictive strain in the direction of the arrows. (The finite thickness of a domain wall is neglected here.).

These effects result in a magnetic after-effect which is analogous to the earlier-mentioned elastic after-effect. For small field strengths, figures 7 and 8 may also be applied to the magnetic phenomenon, substituting the field strength H for the stress σ and the induction B for the deformation ε. Suppose, for example, that a piece of iron, containing a few thousandths percent of dissolved C or N, is placed in a weak magnetic field. When the field is removed, then only a part of the induction will disappear virtually instantaneously; the remaining part disappears gradually at a rate which is again determined by the frequency of movement of the dissolved atoms between sites and is therefore dependent upon the temperature. In an alternating field the magnetic after-effect results in a phase-shift between field and induction, involving a dissipation of magnetic energy which must be added to hysteresis and eddy current losses.

Stability of supersaturated solutions

Ordered solutions (hardening of steel)

If we now return to the earlier mentioned hardening of steel in the middle of an argument on magnetic phenomena in iron, it may seem that we are jumping from one subject to another. This, however, is not the case, for an explanation of the *stability* of hardened steel must be sought in the nature of the interstices in α-iron and their division into x, y and z interstices. The local asymmetrical deformation of the iron lattice which accompanies the introduction of a C or N atom, means that the introduction of a second atom into certain neighbouring spaces of the same group (x, y or z) requires a smaller deformation energy. That is to say, the position into which the second atom must enter has already been slightly stretched by the first atom. Thus the occurrence of highly supersaturated, but relatively stable solutions of C or N in α-iron is conceivable, provided that all theses atoms could be introduced into equivalent interstices (say, the x-interstices). This is precisely what does occur automatically in the hardening of steel. The basic material, iron, containing in addition to other elements, a large amount of carbon, about 1 % by weight, is heated to a temperature at which the metal is in the γ state. On account of its high solubility in the γ phase all the carbon goes into homogeneous solution (cf. fig. 2). The metal is then very rapidly cooled, so rapidly that the segregation into α crystals with little dissolved C and iron carbide Fe_3C, as required by the phase dia-

gram, fails to take place. Instead, something else happens in the neighbourhood of 200 °C. The lattice suddenly changes into the α state, the mechanism being such that after the change all the C atoms are located in one kind of interstice, say the x interstices. The lattice constant in the x-direction is in consequence greatly increased, and in the y and z directions decreased (*fig. 10*). This hard tetragonally-deformed variety of α-iron is known as martensite. Jumps of the carbon atoms between unlike interstices cannot occur on account of the

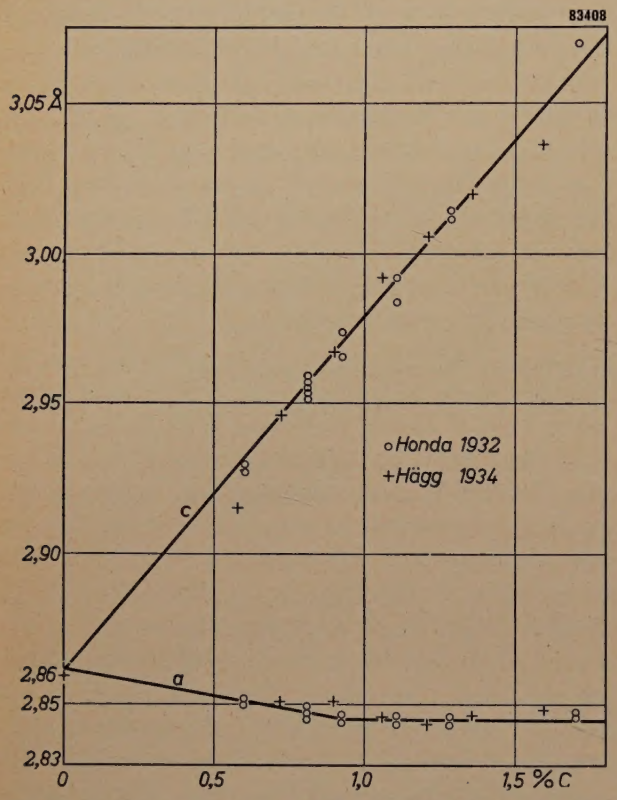

Fig. 10. Lattice constants (a and c) for martensite as a function of the carbon content.

tetragonal deformation and the accompanying co-operative stabilizing action of the carbon atoms. Jumps between like interstices are impossible, because each interstice has unlike neighbours only. Thus a slow precipitation of Fe_3C, such as occurs in disordered supersaturated solutions, in which the carbon atoms make about 1 jump per second at room temperature cannot take place. Old swords still retain their great hardness after many centuries due to this ordered supersaturation with carbon.

A process analogous to that with carbon is likewise possible with nitrogen; the product is then referred to as nitrogen martensite.

Disordered solutions

The precipitation of carbide or nitride which may occur in disordered supersaturated solutions of carbon and nitrogen in α-iron, likewise leads to an increased hardness which remains however far below that attained by the ordered hardening discussed above. One of the reasons for this is that the concentration of carbon or nitrogen is much lower. Precipitation is particularly undesirable if the metal is to be magnetically soft. On account of the decrease in the solubility with decreasing temperature, precipitation can even occur in steel with a very small C and N content. In moving towards a state of equilibrium, there first forms in the supersaturated solution a very fine precipitate, which gradually coarsens, since in this process the total grain boundary surface energy must fall. The precipitate impedes the movement of the domain walls, attaining a maximum effect when the particles of the precipitate are of the same order of size as the thickness of a domain wall (about 10^{-5} cm). The unfavourable influence on the magnetic properties of soft magnetic materials is then appreciably greater than when the same amounts of C or N are present in solution. This gradual deterioration in the magnetic properties is called magnetic ageing. That slowly-cooled mild steel also shows this phenomenon appears to result from the joint presence of manganese and nitrogen [7]). The carbon present precipitates completely during the slow cooling, but the manganese greatly retards the precipitation of the nitrogen The coercive force of mild steel containing a mere 0.005% of N, increases on ageing the steel for a few hundred hours at 100 °C often to twice its former value. The hysteresis losses will therefore also increase. The small amount of nitrogen may be redissolved and the original coercive force restored by heating the metal for a short time at only 250 °C. Ageing will set in anew, however, when the temperature is lowered again.

This undesirable effect can be largely eliminated by adding metals with a strong affinity for nitrogen to the steel. Examples of such metals are aluminium, titanium, zirconium and vanadium. These form stable nitrides AlN, TiN, ZrN and VN. The small magnetic ageing of silicon iron, which is used in large quantities for the construction of transformers, motors and generators seems to be due to the same effect: according to our investigations, the nitrogen present in this metal is fixed in the form of a stable nitride, viz. silicon nitride, by a suitable heat treatment.

Ageing of the type discussed above, based on rapid cooling is called quench ageing to distinguish it from strain ageing discussed earlier. Quench ageing

[7]) J. D. Fast and L. J. Dijkstra, Philips tech. Rev. **13**, 172-179, 1951/52.

likewise manifests itself in the mechanical properties, since movement of the dislocations is also impeded by a precipitate. The maximum hardening effect occurs at a much lower particle size than in the case of the magnetic properties, since the range of action of a dislocation is considerably less than the thickness of a domain wall. This difference is demonstrated in *fig. 11*, which gives a rough indication of the variation of hardness and coercive force of mild steel containing 0.07% of C, which was quenched from 680 °C and subsequently heated for 1 hour at temperatures of 50 °C, 100 °C, 150 °C, 200 °C etc. The data are derived from the measurements of

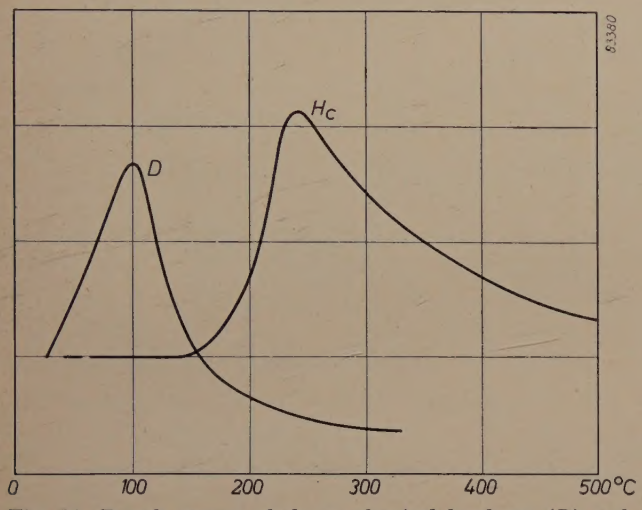

Fig. 11. Rough curves of the mechanical hardness (D) and the coercive force (H_c) for a mild steel containing 0.07% of carbon, after quenching from 680 °C and heating for one hour at the temperatures indicated on the abscissa (from data of Köster [8]).

W. Köster [8]). As may be seen, the maximum mechanical hardness occurs on heating at 100 °C. On heating at higher temperatures, the precipitate is too coarse to have very much effect on the mechanical properties. On the other hand, the maximum influence on the magnetic hardness (coercive force) occurs after heating at 250 °C, when the particles are on the verge of microscopic visibility and their influence on mechanical hardness is negligible.

Transport phenomena in interstitial solutions

In the foregoing examination of the effects of interstitial atoms in metals, attention has been paid particularly to the influence of the strain energy. That the accompanying electronic interaction cannot be ignored even in the simple case of carbon or nitrogen in unalloyed iron, may be seen from experiments on transport phenomena in electric fields. Seith and co-workers [9]) established that carbon in solid iron at 1000 °C moves under the influence of an electric field in the direction of the negative pole, while nitrogen on the other hand moves in the direction of the positive pole. Transport phenomena are shown particularly clearly by oxygen-containing zirconium [10]). In a zirconium wire heated by means of a direct current, the oxygen moves towards the positive pole. At the end adjacent to the negative pole practically pure zirconium is formed. This is indeed the sole method which has been found up to now for purifying solid zirconium of oxygen. Purification by chemical methods is impossible. If the oxygen-containing metal is brought into contact with molten calcium, for example, only a part of the oxygen is removed, since the affinity of zirconium for oxygen increases as its oxygen content decreases. Heating the metal at high temperatures in vacuo to drive off the oxygen is likewise of no avail. Unfortunately the electrolytic method of purification is of no practical significance, since the mobility and the transport number of the oxygen particles are smaller by many orders of magnitude than the mobility and transport number of the conduction electrons. The term particles and not ions is used here intentionally, since the oxygen should not be thought of as clearly distinguishable O^{--} ions. It is merely that the electron gas in the metal is distributed in such a way that the oxygen atoms, on the average have a slight excess of negative electric charge. Experiments so far give the impression that this effective charge on the oxygen atoms in zirconium lies far below one elementary charge.

Also of great interest are the phenomena resulting from the presence of hydrogen in metals. The above discussed strain energy seems to play hardly any part in solutions of hydrogen in metals. For example, the solubility of hydrogen in the body-centred cubic modification of Zr with its small interstices is greater than the solubility in the hexagonal close packed modification which has larger interstices [11]). It is natural to seek an explanation of this in the extremely small size of the hydrogen ion: the radius of this ion (the proton) is but a hundred thousandth of the radius of an atom. Again, one should not think of the hydrogen as present in metals in the form of clearly distinguishable ions; averaged over a sufficiently long time, however, a dissolved hydrogen

[8]) W. Köster, Arch. Eisenhüttenwesen **2**, 503-522, 1928/29.
[9]) W. Seith. Diffusion in Metallen, Springer, Berlin, 1939.
[10]) J. H. de Boer and J. D. Fast, Rec. Trav. chim. Pays-Bas **59**, 161-167, 1940.
[11]) J. H. de Boer and J. D. Fast, Rec. Trav. chim. Pays-Bas **55**, 350-356, 1936.
[12]) A. Coehn and W. Specht, Z. Physik **62**, 1-31, 1930; A. Coehn and H. Jürgens, Z. Physik **71**, 179-204, 1931; A. Coehn and K. Sperling, Z. Physik **83**, 291-312, 1933.

atom will have a deficiency of negative charge. This is in agreement with transport experiments by Coehn and co-workers [12]) who showed that hydrogen in palladium moves towards the negative pole. If the dissolved hydrogen proceeds through the metal lattice in the form of protons, much greater diffusion coefficients are to be expected for this element than for carbon, nitrogen and oxygen. This expectation is borne out by the facts. Thus the diffusion coefficient of hydrogen in α-iron at 20 °C is more than 10^{12} times greater than the diffusion coefficients of carbon and nitrogen [13]). The diffusion coefficient of hydrogen is indeed so large that it might be expected that iron would be permeable to it even at room temperature. The fact that it is possible to store this gas under high pressure in iron cylinders without any perceptible reduction in pressure as a result of diffusion through the walls seems, however, to be in conflict with the above. A similar apparent discrepancy may be seen in the previously mentioned fact that oxygen cannot be driven out of zirconium by heating, even at temperatures at which its diffusion coefficient in this metal apparently has a high value. The explanation of these conflicting observations lies in the fact that the permeability of a metal wall to a gas is often determined not by diffusion, but by a surface reaction. As we have noted on more than one occasion, this explanation is not generally known (publication took place at a rather inopportune moment [14]); it will therefore be briefly discussed below.

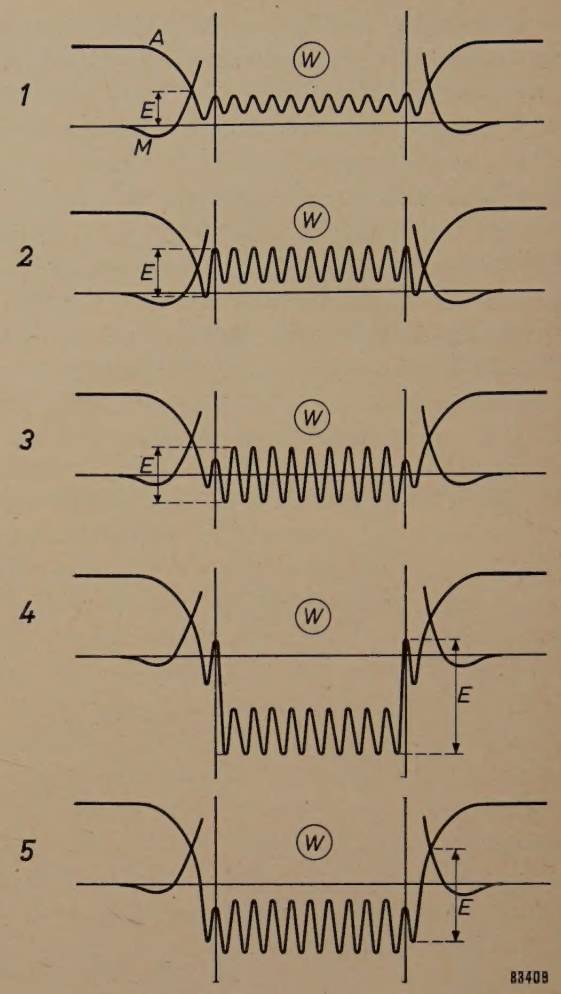

Fig. 12. Schematic representation of the passage of a gas through a metal wall (W). The "potential curves" M and A give the energy of a gas molecule and of its two separate atoms, respectively, as a function of position. The greatest potential jump occurring (E) determines the rate of the whole process. It may occur at any one of five different locations, corresponding to cases *1-5* summarized in the text.

The passage of gases through metals

The passage of a diatomic gas through a metal wall requires five successive processes: 1) the splitting of the molecules into atoms at the surface of entry, 2) the transition of the atoms from the adsorbed state into the interior of the metal, 3) diffusion within the metal, 4) transition of the atoms from the dissolved state into a state of adsorption on the surface of exit, 5) the recombination of the adsorbed atoms into molecules on the surface of exit (*fig. 12*). The slowest of the five processes will determine the permeability. In the passage of hydrogen through an iron wall the first of the five processes, the splitting of H_2 into 2H, is the slowest and is thus the rate determining process. This may be immediately demonstrated by an experiment in which atomic hydrogen is fed to one side of an iron wall. Even at room temperature a ready penetration occurs. If the surface of entry of the iron is made very rough, then the second process, the penetration of the adsorbed hydrogen atoms into the interior, becomes the slowest process. In this case, splitting of the hydrogen molecules into atoms at sharp points and edges takes place spontaneously even at room temperature. The atoms formed are now so much more strongly attached to the surface than is the case for a smooth surface, that the transition to the interior of the metal is rate determining.

In experiments with other gas-metal combinations, instances where the third, fourth of fifth process is rate-determining, have been noted. Thus, for example, diffusion is rate-determining in the passage of hydrogen through a copper wall. Above some hundreds of degrees centigrade, diffusion also determines the rate at which hydrogen passes through an iron wall, in contrast to the situation

[13]) H. D. Fast and M. B. Verrijp, J. Iron and Steel Inst. **176** (I), 24-27, 1954.
[14]) J. D. Fast, Philips tech. Rev. **6**, 365-371, 1941; **7**, 74-82, 1942.

at room temperature. The processes occurring at the surface of exit determine the permeability of a wall of zirconium to oxygen and of a wall of palladium to hydrogen.

To close this necessarily incomplete review on the influence of interstitial atoms in metals let us just return once more to those cases where their presence causes hardness and brittleness in metals. As we have seen, the great hardness of martensite is based on the formation of a new lattice with much smaller interstices, in which the carbon or nitrogen are present under constraint. It is conceivable that hardening could result not only from the formation of new interstices but also from the formation of new atoms. This is actually the case in nuclear reactors using uranium as fuel, and constitutes one of the most urgent metal problems there. The energy production of such a reactor is based on the splitting of nuclei of the isotope U^{235} with the formation of two new atoms. Under the most favourable conditions only one of these atoms can be accomodated in a lattice position, and the other must be taken up interstitially. The ever rising concentration of interstitial atoms eventually causes the uranium rods to break up. One of the tasks of the metallurgist is to prepare uranium in such a state that it can take up as many extra atoms as possible.

THE "DUPLO" CAR HEADLAMP BULB WITH AN ASYMMETRIC DIPPED BEAM

628.971.85:629.113.06

Motorists driving in the dark should dip their headlamps for each oncoming car in order not to dazzle its driver. Dipping is usually done by switching over from the main headlamp filament to an auxiliary filament which supplies the dipped beam. The problem of getting sufficient visibility for safe driving with this limited beam has been tackled from different angles on the continent of Europe and in America.

On the continent the main requirement has been laid on the least possible dazzle. The continental lamps based on this idea give a beam which is symmetrical about a vertical plane through the axis of the lamp and has a sharp horizontal cut-off obtained by means of a small metal cap mounted under the auxiliary filament. In America the emphasis has been laid on the illumination of possible obstacles on the road, the requirement of minimum dazzle taking second place. The asymmetric beam of the so-called "sealed-beam" lamp is based on these premises. This gives more light on the near-side of the road than on the off-side (the off-side is lit by the lamps of the oncoming car). This arrangement gives little consideration for dazzle on bends or the dazzle of cyclists or pedestrians on the near side of the road. This difference between American and continental practice has been described earlier in this Review [1]).

For the motorist, the higher light intensity on the nearside kerb [2]) is an advantage of the American dipped beam. The reduced dazzle of the oncoming motorist and other road users and the sharp light-dark cut-off which helps in the aiming of the beam (which, of course, is very important) are advantages of the continental system.

It is possible to combine the advantages of both systems to a considerable extent by cutting off a part of the metal cap under the auxiliary filament of the continental type of bulb (see *fig. 1*). The dipped deam then obtained retains the sharp light-

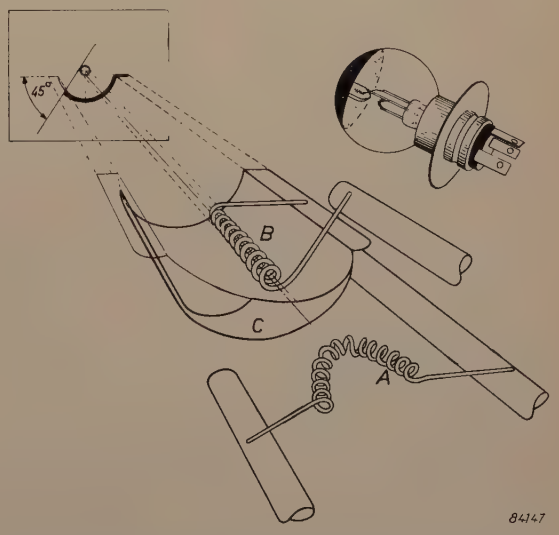

Fig. 1. Main filament *A*, auxiliary filament *B* and metal cap *C*, showing their positioning in a headlamp bulb of the new type. (See right top). The part of the metal cap drawn in thin lines is cut away in order to give the asymmetric beam. This is further clarified in the projection of the metal cap shown in the top left of the figure.

[1]) J. B. de Boer and D. Vermeulen, Motorcar headlights, Philips techn. Rev. **12**, 305-317, 1950/51.

[2]) Note that figs. 1 and 2 relate to lamps developed for those countries where the traffic drives on the right-hand side of the road. A lamp for left-hand traffic can of course be designed on the same principles.

dark cut-off of the original lamp on the off-side but on the near-side more light is radiated so that the beam is here more like that of the American lamps.

Road tests according to internationally approved procedures have shown that the new asymmetric beam lamp gives at least the same visibility as the American sealed beam lamps [1]) (since publication of the article [1]), these have been somewhat modified), and hardly more dazzle than that of the existing con tinental lamps. Because of the latter there can be no objections from a technical point of view to the use of the new asymmetric lamp in countries which approve the existing continental dipped beam.

The light distribution obtained with the new lamps and that with the sealed-beam lamps are compared in *fig. 2a* and *b*. In the direction of points on the right side of the road [2]) in the region 50-200 yds in front of the car, the light intensity from the new asymmetric bulb is about 2/3 that of the new type of sealed beam lamp. In the direction of the eyes of the oncoming motorist, the light intensity of the assymmetric bulb is only 1/3 that given by the American headlamp.

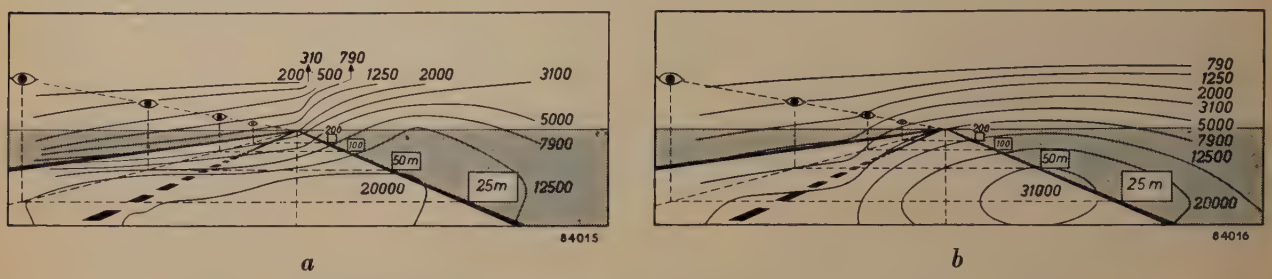

a *b*

Fig. 2. Light distribution [2]) *a*) of the new asymmetric beam European headlamp bulb, *b*) of the latest type of American sealed beam lamp.

The light distributions are here given by iso-candela lines. The six-yard-wide road is viewed from a point midway between the headlamps of a car in the middle of the right half of the road and projected on an imaginary screen in front of the car. In the perspective picture so obtained, each iso-candela line joins the points corresponding to directions in which the light intensity due to both headlamps together has the value marked by the line. Note that the distances are actually given in metres.

J. de BOER.

"BOEKESTEYN"
THE AGROBIOLOGICAL LABORATORY OF N.V. PHILIPS-ROXANE

by R. van der VEEN.

632.931.33:615.777/.779

A number of articles are due to appear in this Review on the work of the Boekesteyn agrobiological laboratory. As the fields of disease and pest control in agriculture and horticulture will be unfamiliar to most of our readers, we have thought it desirable to begin this series with the introductory survey given below.

Protection of cultivated plants

When N.V. Philips-Roxane entered the field of disease and pest control in agriculture and horticulture, it became necessary to have available a laboratory for experimental work in these fields. Such a laboratory has now been established at the old country estate of "Boekesteyn" at 's-Graveland, near Hilversum. The Boekesteyn estate consists of a manor house (*fig. 1*), a fine park, a farm, a kitchen garden with several hothouses, and an orchard of young trees. The park, which is open to the public, is quite separate from the laboratory. The farm is also separate and is let. The house, however, is completely equipped as a laboratory, and the kitchen garden and orchard are likewise turned over to experimental purposes.

It is the aim of the research at Boekesteyn to develop efficient and economic means to combat diseases and pests in all types of cultivated plants. Although in an agricultural country such as the Netherlands intensive measures of disease and pest control have been in progress for a considerable time, at least 10% of the possible harvest is lost as a result of commonly occurring diseases. In most other countries this percentage is considerably higher.

It is sometimes asked why there is so much spraying and dusting nowadays. "There was none of that in the old days, but the fruit still grew on the

trees and there was still corn in the fields", it is argued. That may be so, but to-day much more exacting demands are made as regards the yields par acre and there are many more acres under cultivation. This increased cultivation usually involves a wider spread of diseases and pests.

The plant is a living organism; therefore, by careful selection, a certain resistance can be built up to specific diseases. It would be ideal if exclusively resistant varieties could be raised. Plant improvement laboratories and institutes are indeed busy with the breeding of such races and much has already been achieved in this field. The enemies of the plant, for the most part fungi and insects, are likewise living organisms, however, and show great adaptability. As a consequence it is often found that a few years after a plant, resistant to a certain fungus, has been cultivated on a large scale, the fungus has also produced a new variety which is adapted to the improved plant. Therefore, for the time being at least, the employment of chemical protective measures remains necessary.

It goes without saying, however, that injudicious use of these chemical agents may well lead to results just the reverse of those expected. A good example of this was the large-scale spraying of citrus plantations with DDT which was carried out at a time when it was still considered that DDT was effective against all insects. There was, however, a scale which was unaffected by DDT. Its enemies were exterminated by the spraying, so it was able to multiply unhindered. The damage wrought by this single species was greater than that which would have been caused by all the other pests together had there been no spraying!

Other examples might be cited which show how the balance of nature may be disturbed by spraying. But here it should be remembered that agriculture itself is a disturbance of the balance of nature. It begins whenever the original vegetation is rooted out and a new form of vegetation is artificially cultivated in its stead. Only by hard work can the farmer maintain this disturbance.

Fig. 1. Boekesteyn House, now fitted out as an agrobiological laboratory for Philips-Roxane.

Better manuring brings new weed problems, more productive varieties frequently have new susceptibilities, extension of the area under cultivation brings with it more virulent diseases and pests. Chemical measures against diseases have their drawbacks, but they are nevertheless essential in a densely populated world.

One of these drawbacks has already been named: not only the parasites, but also the parasites' enemies may be exterminated by chemical agents and the chance of a rapid spread of a new plague is thereby increased. Another danger is that substances toxic to insects are often harmful to man also. The

further development of agricultural chemicals must therefore be directed towards the discovery of substances which are not toxic to man and are selectively toxic to the pests, leaving all other insects undisturbed.

This means that the substance must have a highly selective action. The ideal solution would be to have available a series of substances, each active against one particular type of harmful insect without being poisonous to other creatures. Something of a similar nature would be desirable for fungous diseases; here, however, a substance will suffice which is harmless towards green plants and animals, but active against all fungi.

Before going further into this ideal objective, it is necessary to give a brief review of the development of chemical disease and pest control over the course of the years.

Chemical agents for combating plant diseases and pests

Plant diseases are caused by fungi, by bacteria or by viruses. Moreover, plants are exposed to insect pests and the encroachment of weeds.

A whole arsenal of chemical agents is available for combating all these evils except the virus diseases. For opposing the latter we are still wholly dependent upon the selection of resistant varieties and on the rigorous weeding-out of infected plants and other measures for reducing the danger of contagion.

We will here limit ourselves to the methods by which fungous and bacterial diseases and insect and weed pests may be combated.

Fungous diseases

In general, fungi propagate themselves by means of spores. Therefore, the spread of the disease can be controlled by an agent which will kill the spores or prevent them from germinating.

Various substances (fungicides) are known which operate in this way. The oldest agent and one which is still very widely employed is Bordeaux mixture, a mixture of copper sulphate and lime. To-day there are various other copper compounds on the market which are equally effective, for example, copper oxychloride and the so-called "colloidal copper". Mercury compounds have also made progress, especially as seed desinfectants; they are less suitable for field use, being frequently injurious to plants. There are, however, organic mercury compounds which can be used for spraying fruit trees, although a certain degree of caution must be exercised.

In the last 15 years important applications have been found for organic compounds containing no toxic metals like copper and mercury. The dithiocarbaminates and the quinones in particular have furnished a number of excellent fungicides.

Dithiocarbaminates. Unlike bacteria, most fungi appear to be sensitive to certain dithiocarbaminates, for example tetramethylthiuram disulphide [1] [1]) — known as TMTD — and zineb [2].

Even when diluted to $1 : 10^6$ in water, these compounds completely prevent the germination of spores. A plant which has been sprayed or dusted with them is thus very well protected against most fungous diseases. These compounds are gradually replacing the copper and mercury compounds.

Quinones. Among the quinones, compounds are found [3], [4] whose fungicidal action is of about the same intensity as that of the compounds of the previous group. Their price, however, is somewhat higher and as a consequence they are gaining less ground than the dithiocarbaminates.

Latterly, yet another organic fungicide, known as captan [5], has come to the fore. In general, it is perhaps of a somewhat lesser fungicidal value than the dithiocarbaminates, but it has the favourable property of appreciably improving the colour of both leaves and fruit when used on fruit treess. For the fruit this means a higher market value and for the leaves a longer period of assimilation extending into the autumn, and hence a more vigorous growth of the tree. Philips-Roxane have developed a very useful fungicide which likewise enjoys this property, possibly to an even higher degree.

Frequently the resistance of a plant to fungal diseases rests upon the fact that the plant contains some substance toxic to the fungus. If growers could introduce such substances into their plants artificially, it would be possible to achieve resistance in this way. The substance must be such that the plant may assimilate it and distribute it throughout its whole system without suffering any resultant damage. Such substances are known as "systemic" fungicides.

A few substances are known which have a clearly systemic action, but not one of these however, has been developed far enough to find practical application. Nevertheless, an intensive search for systemic fungicides is in progress at Boekesteyn. A great advantage of such a fungicide would be that, on being sprayed solely on the leaves, it would be distributed throughout the whole plant and would thus also protect the roots against ground fungi.

[1]) The numbers in square brackets placed after the names of the compounds refer to the corresponding structural formulae given in the appendix.

Bacterical diseases

Bacterial diseases are usually more difficult to combat than those caused by fungi, since the bacteria spread throughout the soil and infect the plants via the roots. Disinfection of the soil is the best treatment available, but is expensive.

In recent years antibiotics such as streptomycine have been employed as "systemic" agents against bacterial diseases, sometimes with success. They render the plants less susceptible to bacteria, but the price and often the toxicity to the plant form obstacles to their general application.

Insect pests

The increasingly intensive cultivation of the land in the present century has led to a marked increase in the number of insect pests. Insects, it appears, quickly adapt themselves, and on being offered many acres of food, will propagate themselves with extraordinary rapidity.

Like fungi, insects were formerly combated with inorganic poisons, such as lead arsenate and copper arsenite. In the last ten or twenty years, changes have occurred also in this field.

It was first found that some plants contain substances which are extremely poisonous to insects: nicotine from tobacco, rotenone from Derris, pyrethrine from Pyrethrum. Tobacco, Derris and Pyrethrum were specially cultivated for the production of these substances.

Since 1940 these substances are no longer used on such a wide scale, owing to the discovery of extremely efficient insecticides which can be produced synthetically at low cost.

Dichloro-diphenyl trichloroethane [6] — widely known as DDT — was the first, and rapidly gained general acceptance when it was observed that many insects were susceptible to it and that warm-blooded animals could tolerate large doses of it. DDT has given good service in combating malaria and typhus.

Hexachloro-cyclohexane [7] (known as HCH or BHC) followed shortly afterwards and appeared to be more toxic to many insects which are insensitive to DDT. One disadvantage of HCH, however, is its unpleasant smell. Further research showed that HCH consists of a mixture of isomers and that it is the gamma-isomer almost exclusively which is responsible for the insecticidal properties; this isomer is odourless. The gamma-isomer is produced by Philips-Roxane under the name of lindane (called after Van der Linden, who was the first to isolate the gamma-isomer in the pure state).

More recently a new group of insecticides is gaining ground (aldrin [8], dieldrin [9]).

Substances extremely toxic to insects were found during war-time research on poison gases. Several of them (for the greater part phosphorus compounds) have rapidly gained ground in agriculture. The best known of these is parathion [10]. A disadvantage of such materials is that they are toxic not only to insects but also to all animals and thus also to man. However, insecticides have more recently been discovered in this group which are less toxic to warm-blooded animals, for example, malathion [11].

Just as substances are being sought which render the plant itself poisonous to fungi or bacteria, so also a search is in progress for "systemic" insecticides. Several compounds from the above-named group of phosphorus compounds show this effect, that is to say they are assimilated by the plant without causing it any damage and thereby render the plant toxic to insects which feed upon it; an example of this is schradan [12]. Since these substances are broken down only slowly in the plant, the treatment of plants intended for human or animal consumption must take place a long time before they are due to be eaten, since the systemic insecticides are also very poisonous to man.

Spider mites (Acaridae) are also very harmful to plants. Although these creatures are not insects, but members of the spider family, the agents used to combat them (acaricides) are usually considered as insecticides. Normal insecticides as a rule have little effect on mites; DDT appears indeed to exert a stimulating influence upon them. Parathion, which is fatal to all animals, does, however, exterminate mites; as do also mineral oils. Philips-Roxane has developed a further acaricide which will come into production in 1955. Its toxicity to insects is so low that bees, for example, may be fed upon it without suffering any harm.

Weed pests

It is curious that substances which must be classified as belonging to the group of "growth-hormones" (further details regarding which will be published in a later article) may also be employed to effect the antithesis of growth, namely to eradicate certain plants. Thus the widely-known compound, 2,4-D [13], will kill most dicotyledons in certain concentrations but will leave monocotyledons unharmed. With this substance, therefore, meadows and cornfields may be rendered free from weeds.

Two other weed-killers (herbicides) based upon growth-hormones, namely 2,4,5-T [14] and 2-methyl-4-chloro-phenoxy-acetic acid [15] — known

as MCPA — have an analogous action. However, their effects differ: brambles and nettles may be combated with 2,4,5-T, while 2,4-D and MCPA have little effect upon these weeds.

Weed-killers are also sought which will selectively kill grasses while leaving dicotyledons unharmed. Up till now, however, this search can hardly be said to have been successful. There is a preparation which is known as a "weed killer for carrots", which will kill all plants, save only the umbellifers and the majority of conifers, so that it can be used on carrots and celery and in coniferous nurseries.

Finally we must mention a group of compounds which exterminate all plants and are used, for example, in keeping paths free from overgrowth. For this purpose, certain types of chlorates or arsenic compounds are employed and sometimes also pentachlorophenol [16], known as PCP. Various new compounds for this type of application, e.g. trichloroacetic acid (TCA) [17] and chlorophenyl dimethyl urea (CMU) [18] are still in the experimental stage.

Agrobiological research at Philips-Roxane

Agrobiological research work at Philips-Roxane is pursued along the following broad lines:

1) By investigating the natural chemical defensive agents in plants, an attempt is being made to gain an insight into the mode of operation and the character of those substances which nature, as it were, has provided to make plants resistant to fungi and insects.
2) By a search for "systemic" chemicals, such as are harmlessly assimilated by plants, attempts are being made to increase the resistance of plants to certain diseases or to render them toxic to certain insects.
3) By testing numerous substances for their effect on fungi, insects and the higher plants, it is hoped to find compounds with as little toxicity as possible to man and the domestic animals; such substances must be as selective as possible so as to kill a very definite class of insects but be non-injurious to other insects.

Research at Boekesteyn is conducted by five departments which are in close contact with the Philips-Roxane chemical laboratory at Weesp. In the latter laboratory new chemical compounds are synthesized and are later tested at Boekesteyn.

The departments at Boekesteyn are as follows:

a) The entomological department, where compounds are tested for their insecticidal properties.
b) The mycological department, where the same process is carried out with respect to fungicidal properties.
c) The systemic department, where systemic fungicides and the naturally occurring defensive agents of plants are studied.
d) The herbicide department, which investigates the concentrations of compounds injurious to green plants.
e) The field service, which conducts field tests on substances which have given promising results in the laboratory.

A substance received for investigation usually undergoes examination roughly as follows. It is first ascertained in the entomological and mycological departments and sometimes also in the systemic department, whether small concentrations of the substance are lethal to insects or fungi. Various species of insects and fungi are employed for this purpose; this means that an extensive collection of these species has to be maintained in culture (*fig. 2*). If the compound appears to be active when very highly diluted, then it is sprayed onto plants for the purpose of ascertaining whether the latter suffer any damage from the compound — this is all too often the case. If, however, the plant is much less susceptible than the fungi or insects (the susceptibility

Fig. 2. Breeding of flies, which are used for initial tests on new disease and pest control substances.

must be at least a hundred times less), then there is here a case for further research. This consists in the first place in accurately determining the concentration necessary to give 50% mortality first for fungi or insects and then for the plants. Here the investigation extends over a greater range of fungous and insect species than in the previous test.

If after all this, the compound still appears to show promise, an investigation follows into its toxicity to warm-blooded animals and a few experiments are conducted with it in the field.

If the possibilities still appear favourable, the feasibility of industrial-scale production is examined. This involves the following: choosing the simplest method of production, calculating the cost price, carrying out "formulation" tests (i.e. tests to ascertain the form in which the compound can be best employed: as spraying powder, as dusting powder, as emulsion, etc). and an exhaustive investigation by means of field tests to ascertain those diseases or pests against which the compound is effective; finally permission to market the compound for specific uses must be sought from the competent authorities of the various countries (such applications are directed in the Netherlands to the Director General of Agriculture via the Plant Disease Service).

As may well be imagined, only a very small number of the hundreds of compounds which are sent each year from Weesp to Boekesteyn satisfactorily pass through all stages. The overwhelming majority get no further than the first test for killing properties, and of the few which pass through this stage, many fall by the wayside during the later investigations. The very few exceptions which do come to fruition must atone for the many disappointments.

APPENDIX: STRUCTURAL FORMULAE

Below are given the structural formulae of the compounds mentioned in the text.

Fungicides

Dithiocarbaminates

[1] TMTD . . . . . 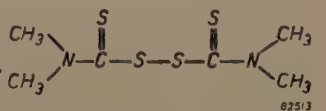

[2] Zineb . . . . . 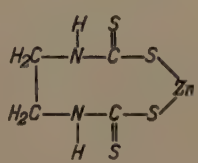

Quinones

[3] Dichloronaphthaquinone . . . . . 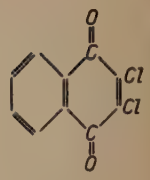

[4] Tetrachlorobenzoquinone . . . . 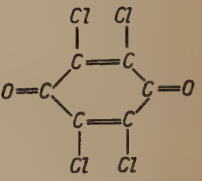

[5] Captan . . . . . 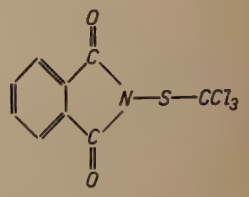

Insecticides

[6] DDT . . . . . 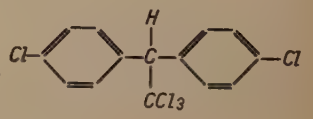

[7] HCH. BHC, Lindane . . . . . 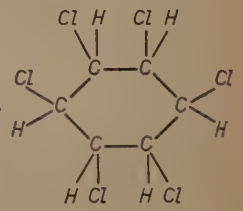

[8] Aldrin . . . . . 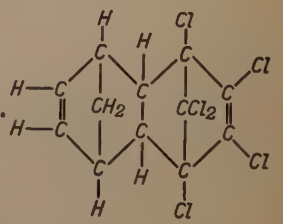

[9] Dieldrin . . . . . 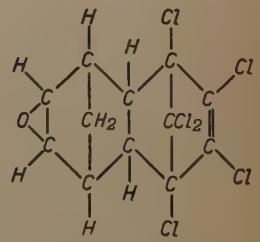

[10] Parathion . . . . . 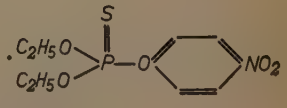

[11] Malathion . . . .

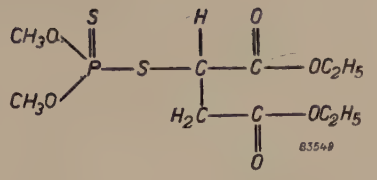

[12] Schradan (systemic insecticide) . . . . . .

. . . . . .

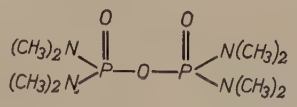

Herbicides

[13] 2,4-D . . . . . .

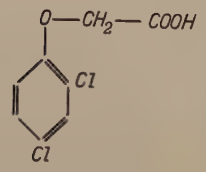

[14] 2,4,5-T . . . . . .

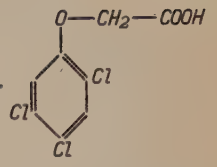

[15] MCPA . . . . . .

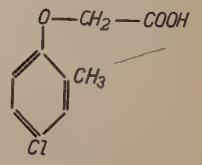

[16] PCP . . . . . .

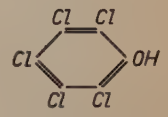

[17] TCA . . . . . CCl_3-COOH

[18] CMU . . . . . .

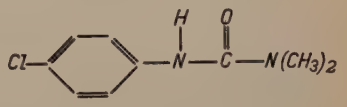

Summary. This article forms the introduction to a series of articles on the work of the "Boekesteyn" agrobiological laboratory of N.V. Philips-Roxane. This work consists in investigating compounds produced in the company's chemical laboratory at Weesp (Holland).

It is pointed out that the intensification of both agriculture and horticulture in the present century has made the control of diseases and pests more necessary than ever. Chemical agents have a large part to play in this control. Means of control against fungous and bacterial diseases (no chemical agents are yet known against the virus diseases) and against insect and weed pests are reviewed. The organization and departments of Boekesteyn are then outlined (entomological, mycological and "systemic" departments, together with a field service for practical evaluation). A description is given of the procedure followed in investigating the various substances. An appendix is given containing the structural formulae of many of the substances mentioned.

FAST COUNTER CIRCUITS WITH DECADE SCALER TUBES

by E. J. van BARNEVELD.

621.385.832:621.318.57

*The E1T scaler tube *) is a decade scaler within very small compass — a tube no larger than an ordinary radio valve. It has the further advantages of direct reading (the number counted appears as an illuminated spot opposite the digit on the tube) and a high counting rate when used with a suitable input circuit. Suitable circuits, together with the counting rates actually attained by them during laboratory tests, are discussed in the present article. In particular, the counting of random pulses is considered.*

The need for fast scalers, in particular as a means of measuring radioactive radiation and other phenomena associated with nuclear physics, has increased considerably in recent years. Radiation intensities can be measured by means of a Geiger-Müller counter tube [1]), in which every incident particle (e.g. β particle) causes a discharge and so produces an electric pulse, or with a scintillation counter, containing a fluorescent substance which scintillates under radioactive radiation, the scintillations being converted into electric pulses by a photo-multiplier [2]).

Fig. 1. The E1T decade counter tube. A blue-green fluorescent spot indicates the digit corresponding to the position of the beam in the scaler tube, that is, to the number of pulses counted.

Provided that the repetition rate of these pulses is not too high (i.e. does not exceed 100 per second), they can be counted with a simple mechanical counter. Where the pulses follow one another more rapidly, however, it is necessary to employ electronic methods. These methods enable very fast scalers to be constructed. However, if such a scaler be equipped entirely with standard electronic tubes, it will be rather expensive and will require quite a large number of tubes, particularly if it is to be used for decade counting.

Here, the decade scaler tube *) E1T (*fig. 1*), already described in this Review [3]) and in other publications [4]), offers a better solution. Although the functioning of this tube is fully described in article [3]), referred to in the following as I, a brief description of it will now be given.

Operation of decade scaler tube E1T

The E1T scaler tube, shown in cross-section in *fig. 2a* and diagrammatically in fig. 2*b*, is in essence a cathode-ray tube, whose electron gun produces a ribbon-shaped beam (the advantages of which are described in articles [3]) and [4])). This beam can be deflected to and fro by varying the potential of the right-hand deflector plate (D'). Beyond the deflector plates, the beam impinges upon the so-called slotted electrode (g_4), which has ten vertical slots. As the beam traverses this electrode, a certain number of the beam-electrons (depending on the position of the beam) pass through a slot and strike the anode of the tube, which is behind the slotted electrode. The slots are so designed as to produce a variation of the anode current (i_{a_2}) depending on the potential of deflector plate D' roughly in accordance with curve I in *fig. 3*. Since the anode current is virtually independent of the anode potential, curve I is likewise valid when the anode is connected direct to D'. Now, if a_2 and D' are connected to the 300 V line via a common resistor, the potential of a_2 and D' will be:

$$v_{D',a_2} = V_B - i_{a_2} R_{a_2} \quad \ldots\ldots\ldots \quad (1)$$

*) The E1T, previously referred to as a "counter tube", is now termed a "scaler tube" to preclude confusion with counter tubes such as Geiger-Müller tubes etc.

[1]) See e.g. N. Warmoltz, Philips tech. Rev. **13**, 282-292, 1951/52.

[2]) See e.g. H. Dormont and E. Morilleau, Le Vide **8**, 1344-1352, 1953 (No. 45); R. Champeix, H. Dormont and E. Morilleau, Philips tech. Rev. **16**, 250-257, 1954/55

[3]) A. J. W. M. van Overbeek, J. L. H. Jonker and K. Rodenhuis, A decade counter tube for high counting rates, Philips tech. Rev. **14**, 313-326, 1952/53.

[4]) J. L. H. Jonker ,Valves with a ribbon-shaped electron beam; contact valve, switch valve, selector valve, counting valve, Philips Res. Rep. **5**, 6-22, 1950. J. L. H. Jonker, A. J. W. M. Overbeek and P. H. de Beurs, A decade counter valve for high counting rates, Philips Res. Rep. **7**, 81-111, 1952,

This relationship is represented by line *II* in fig. 3, viz. the load line. The points of intersection of lines *I* and *II* represent equilibrium states. It will be seen, however, that only the points in the diagram indicated by dots correspond to *stable* positions of the beam.

In each of the ten stable positions, a certain number of the beam electrons pass through an aperture in the anode and strike a layer of fluorescent material (l, fig. 2*a*) on the wall of the bulb, thus producing a luminous spot to indicate which of the ten stable positions, marked 0 ... 9, is occupied by the beam.

The actual counting process may be described in the following manner. With the beam in a stable position, each count pulse gives rise to a positive voltage step of 14 V which is applied to the left-hand deflector plate (D). Owing to the presence of stray capacitances, the potential of the right-hand deflector plate cannot change so very quickly, and may therefore be considered constant, at least for the time being. Hence the beam shifts abruptly to the left, that is, to the next stable position. If the potential of the left-hand deflector plate be returned gradually to its original level, the stray capacitances will be charged in the meantime, thus enabling the beam to stabilize itself in the new position.

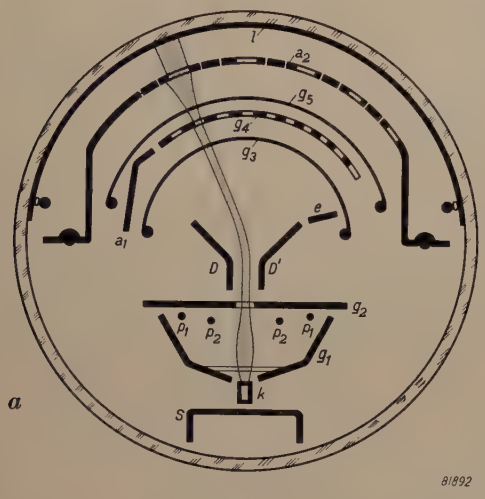

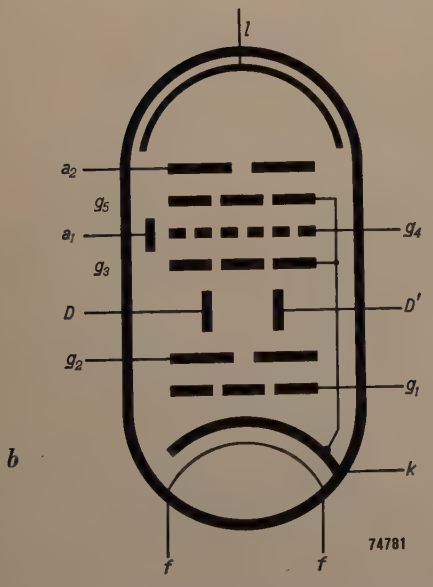

Fig. 2. *a*) Cross-section and *b*) Schematic representation of the decade scaler tube. The cathode (k) (with heater f), the control grid (g_1), the four internally connected focusing electrodes (p_1 and p_2) and the accelerating electrode (g_2) constitute the electron gun, which produces a ribbon-shaped beam (the width of the ribbon is normal to the plane of the drawing). D, D' deflector plates; g_3, g_5 suppressor grids; a_1 reset anode; g_4 electrode with ten slots; a_2 anode; l fluorescent layer; s screen (connected internally to k) preventing primary electrons from striking the tube envelope. The auxiliary anode e (connected internally to g_2) captures secondary electrons.

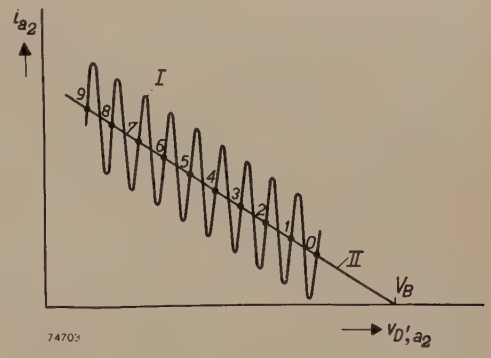

Fig. 3. Undulating line *I*: characteristic of the decade counter tube (anode current I_{a_2} versus potential V_{D',a_2} of the right-hand deflector plate and the anode).
Line *II* is the diagrammatical equivalent of equation (1). Only those points of intersection of *I* and *II* that are numbered from *0* to *9* represent stable beam positions; all others corresponding to unstable positions.

Starting from the extreme right-hand position (0), the beam after nine similar movements, reaches the extreme left-hand position (9). With the tenth pulse it must return to position 0, at the same time causing the beam of another counter tube, counting the tens, to move from 0 to 1. The re-set from 9 to 0 is initiated by the so-called reset anode (a_1, fig. 2*a*): one of the methods of resetting the tube is described in article I, page 323.

The counting of random pulses

A circuit to count 30 000 pulses per second is described in article I: it was there assumed implicitly that the pulses were periodic. However, it is often necessary to count completely random pulses, as in the case of a Geiger-Müller or scintillation counter. Almost all practical cases are covered by these two extremes.

Pulses belonging to the latter group can be counted mechanically or electrically, but in either case a fraction of the pulses produced will escape detection. In the decade scaler tube, for example, the beam requires a certain time to pass from one position to the next; during this time the tube is inactive and any pulses that happen to arrive will not be counted. Similar losses occur in all electronic scalers and the losses are even more serious in mechanical counters. This counting loss depends on the time required by the scaler to record one digit, that is, on the so-called dead-time. Hence it is usual to specify this characteristic property of a scaler.

However, in trying to do so in the case of the tube E1T we encounter a difficulty, i.e. that this tube has two dead-times, namely what may be described as the "step-time" (τ_s), or time required for stepping the beam from one position to the next (0-1, 1-2, ... 8-9), and the "reset time" (τ_r), required to reset the beam from 9 to 0. In general, τ_r exceeds τ_s. In the case of periodic pulses, the counting rate is limited only by the longer of the two dead-times, that is τ_r; if the interval between successive pulses is shorter than τ_r the tube will not operate. However, a more complex situation arises in the case of random pulses.

To understand this, consider pulses distributed entirely at random, and let n represent the average number of pulses recorded per second during a particular count. On the average, then, n will also represent the number of times per second that the counter is inactive. In nine out of every ten cases, the cause of this inactivity is a step, i.e. 0-1, 1-2, ... 8-9, with its associated dead-time τ_s, and in only one of the ten cases is it the reset 9-0, with dead-time τ_r. It will be seen, then, that on an average, the counter is inactive for a time $\tau = (0.9\, n\tau_s + 0.1\, n\tau_r)$ second per second, i.e. it is able to count during only $(1 - \tau)$ second in each second.

Accordingly, the number of pulses actually arriving per second is not n, but:

$$N = \frac{1}{1-\tau} n. \quad \ldots\ldots \quad (2)$$

Here, then, we have what may be described as an average dead-time τ_m:

$$\tau_m = \frac{\tau}{n} = 0.9\, \tau_s + 0.1\, \tau_r. \quad \ldots \quad (3)$$

Now, τ_s and τ_r are of the same order of magnitude: $\tau_s = 24$ μsec, $\tau_r = 27$ μsec [5]); therefore τ_s contributes considerably more than τ_r. We find that:

$$\tau_m = 0.9 \times 24 + 0.1 \times 27 = 21.6 + 2.7 = 24.3 \text{ μsec.}$$

which turns out to be smaller than τ_r. However, this by no means implies that it would be possible to count, on an average, more than 30 000 random pulses per second, as will be seen from the following. From equations (2) and (3): $n = N/(1 + N\tau_m)$. Substituting $\tau_m = 24.3$ μsec and $N = 30\,000$ pulses/sec, we find that $n = 17\,300$ pulses/sec; hence the loss is no less than 42 %.

Such a loss cannot be accepted. Ideally, in fact, the loss should be negligible, e.g. 1%, but the number of pulses that can be counted per second is then relatively small. To illustrate this point we have, from formula (2):

$$n = \frac{1}{\tau_m} \cdot \frac{N-n}{N} \quad \ldots\ldots \quad (4)$$

where $(N - n)/N$ represents the relative loss. It is seen, then, that n is proportional to the loss. If the loss be limited to 1% and if τ_m be 24.3 μsec, we find that $n = 411$ pulses/sec and $N = 1.01\, n \approx n$.

From formula (4), we see that if the number of pulses per second be increased, the loss will also increase, thus necessitating the use of a correction factor to calculate the real quantity (N) from the quantity recorded (n). It can be derived from (2) that this correction factor is $1/(1 - \tau)$, which, in conjunction with formula (3), gives:

$$N = \frac{1}{1 - n\,\tau_m} n. \quad \ldots\ldots \quad (5)$$

The count n can be corrected, employing the correction factor to an extent consistent with the accuracy of τ_m, since the error in the final result arising from any inaccuracy in τ_m is all the larger, the larger the correction factor $1/(1 - n\tau_m)$. In fact, if Δ be the accuracy of τ_m, and δ the required accuracy of N (both in %), it is necessary to satisfy the following condition:

$$n\,\tau_m \leqq \frac{\delta}{\Delta + \delta}.$$

For example, given that the required $\delta = 1\%$ and $\Delta = 10\%$, then $n\tau_m$ must not exceed 1/11. Accordingly, n may be increased to $1/(11\ \tau_m) = 3740$ pulses per sec. It will be seen from the above that even a moderate degree of accuracy in the determination of τ_m is sufficient to procure an increase of a factor of ten in the count rate.

However, if the loss is to be limited to 1% to enable the correcting factor to be dispensed with, but a count rate of about 400 pulses/sec is considered inadequate, it will be necessary to find a means of shortening the average dead-time τ_m. It will be evident that, at all events as far as random pulses are concerned, we should consider primarily the possibility of shortening the beam step-time (0 to 9) rather than the reset time, which contributes only 2.7 to the total of 24.3 μsec.

Now, the "step-time" τ_s may be divided into two parts, i.e. one governed by the scaler tube itself (in a given circuit), and one governed by the pulse shaper (that is, the circuit preceding the scaler tube, whose function is to convert each applied pulse into one of constant shape and

[5]) In article I, page 324, an average value of 27.2 μsec is specified, with due regard to the different safety margins. This value is here rounded off to 27 μsec.

amplitude suitable for counting). Let us now consider to what extent it is possible to shorten τ_s by employing an improved pulse shaper.

Improved pulse shaper

Fig. 4 is the circuit diagram of a pulse shaper able to shape pulses arriving at a higher rate than the corresponding unit described in article I (fig. 20). The circuit itself is fully described in another publication [6]).

It will be seen that fig. 4 is divided into two parts, i.e. the "squarer" (A), to convert the input signal (pulsating, sinusoidal, or square) into square pulses, and the actual pulse shaper (B), to convert the squared pulses into triangular ones.

The square pulse thus produced at P is differentiated in unit B by a combination of a capacitor (C_4) and a resistor (R_{13}). A diode (d_1) prevents the occurrence of any negative peak (corresponding to the jump from 173 V to 130 V), and another diode (d_2) passes the positive peak (resulting from the jump from 130 V to 173 V), which then produces an increase in the cathode voltage of d_2 (point Q) from 156 V to about 170 V.

Given a suitable choice of the time constant C_4R_{13}, it is possible to make the anode voltage of d_2 decrease faster than the cathode voltage, thus driving this valve beyond cut-off. From then on, the potential at point Q will decrease exponentially to an asymptotic value of 90 V, by reason of the

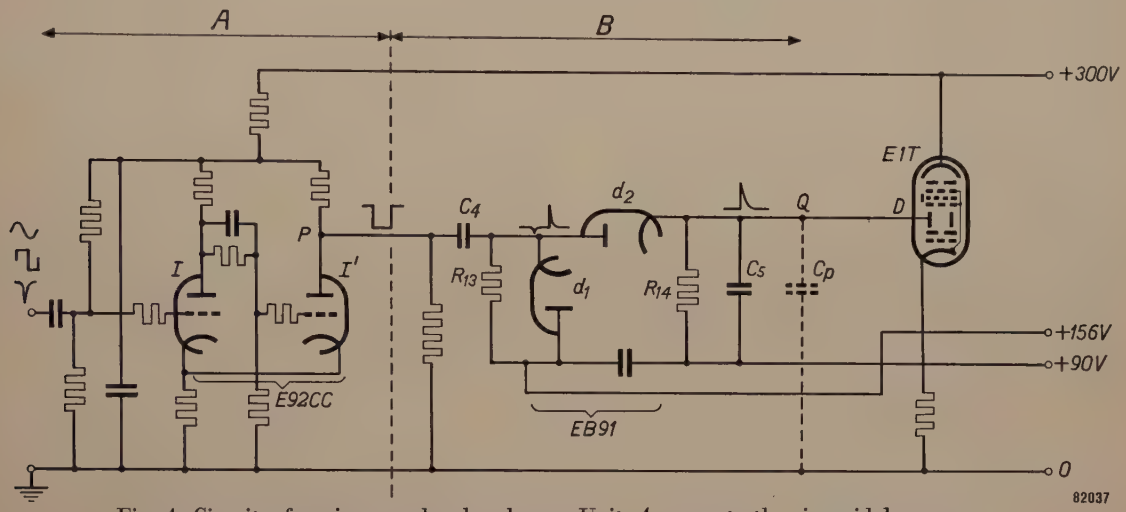

Fig. 4. Circuit of an improved pulse shaper. Unit A converts the sinusoidal, square, or pulsating input signal into square pulses at point P. Unit B differentiates these square pulses which are applied via point Q to the left-hand deflector plate (D) of scaler tube E1T. Section I of double triode E 92 CC is conductive, and section I' non-conductive, in the steady condition. A drop in the grid potential of section I reverses this situation, and a subsequent rise in potential restores it. C_4-R_{13} is a differentiating network. Section d_1 of double diode EB 91 cuts off the negative pulses, and section d_2 passes the peaks of the positive ones. $(C_5 + C_P)R_{14}$ is the time constant of the trailing edges of the pulses occurring at Q (C_P stray capacitance).

The principal component of unit A is a double triode E 92 CC, of which one section (I) is conductive and the other (I') non-conductive, in the quiescent condition; the anode voltage of section I' is then 173 V.

A negative pulse arriving on the grid of section I will drive this section beyond cut-off, and make section I' conductive for the duration of the pulse. During this pulse, then, the anode voltage of section I' will decrease to 130 V, and after it the original condition of the tube will be restored. Accordingly, the potential of point P in the circuit (see fig. 4) drops first from 173 V to 130 V, and then returns to 173 V.

fact that capacitor C_5 (together with the stray capacitances in parallel with it) discharges across resistor R_{14}. However, as soon as the decreasing potential reaches 156 V (that is, the anode voltage of d_1), diodes d_1 and d_2 become conductive again, thus maintaining the potential of point Q constant at or near this value. Since it is small, the voltage drop from 170 V to 156 V is virtually linear, as will be seen from *fig. 5*. Given certain values of C_5 and R_{14}, the base-width of the triangular pulse, with an amplitude of 14 V, thus produced is 13 μsec; such a pulse is suitable for the E1T scaler tube. This enables us to connect point Q to the left-hand deflector plate D (fig. 4).

The dead-time to be taken into account in the counting of random pulses is:

$$\tau_m = 0.9\,\tau_s + 0.1\,\tau_r = 11.7 + 2.7 = 14.4\ \mu\text{sec}.$$

[6]) R. van Houten, A decade counter stage with a counting rate of 100 000 pulses per second, Electronic Appl. Bull. **15**, 34-43, 1954, fig. 3.

Assuming that a 1% loss is acceptable, it follows from (4) that $n = 10^{-2}/14.4 \times 10^{-6} = 695$ pulses/sec, that is, a counting rate much higher than that calculated above.

Again, the question arises whether even an average counting rate of 695 pulses/sec is high enough. However, it will be seen from the following argument that this average is at all events of the correct order of magnitude for many cases.

Fig. 5. Oscillogram of a pulse produced at point Q (fig. 4) by a 50 000 c/s A.C. voltage applied to the input of the pulse shaper. Amplitude 14 V, duration 10 μsec.

If N is to be measured accurately to within 1%, the total number of pulses counted will have to be large enough to ensure that the natural fluctuation (which is completely independent of the dead-time of the scaler) does not produce any error greater than 1%; the minimum total pulse count required to satisfy this condition is 10 000. Moreover, it will then be necessary to measure the actual counting time accurately to within 1%; the shortest counting time that can be measured with a stopwatch with this accuracy is 20 seconds. Now, although the fact that at least 10 000 pulses must be counted in at least 20 seconds does not necessarily imply that 10 000/20 = 500 is either the precise, the average, or the maximum number of pulses per second that the scaler must be able to record. It does imply, however, (assuming a count accurate to within 1%) that this is the correct order of magnitude. In general, there is little to be gained by extending the count beyond a total of 10 000 pulses, since the extension required to produce any essential increase in counting accuracy would be enormous.

In the case of radioactive radiation so intense as to produce more than 10 000 pulses in 20 sec, it is usually possible to compromise either by increasing the distance between the sample and the counter, or by employing a diaphragm. However, such measures are sometimes undesirable, as in the case of coincidence circuits. In these circuits two or more scintillation counters are connected such that a count is recorded only when both counters are struck by the same elementary particle. The number of such coincidences may be expressed as a fraction of the total number of particles striking one of the counters in the same period. This fraction may be very small. Where it is necessary, owing to the low counting rate of the scaler, that the number of pulses per second be kept relatively small, coincidences will be so rare that adequate accuracy can be ensured only by counting over a very long period. Accordingly, such measurements require scalers capable of an average counting rate much higher than some hundreds of pulses per second (assuming a loss of 1%). The same holds good for the counting of a wide variety of effects whose rate of repetition is not controllable.

Hence it is well worth while to examine the possibility of shortening the step-time τ_s still further.

Reducing the contribution of the scaler tube to the step-time

The electron beam in the scaler tube is advanced one step at a time by a count-pulse, that is, a sudden rise in the potential of the left-hand deflector plate (D, fig. 2). Owing to the stray capacitance of the interconnected anode (a_2) and right-hand deflector plate (D'), the change in the potential of these electrodes is relatively slow. After each step of the beam in the left-hand direction, the trailing edge of the pulse takes effect, i.e. the potential of the left-hand deflector plate gradually returns to its original level, so gradually, in fact, as to enable the beam to remain in the new position.

At the same time, the potential of the anode and the right-hand deflector plate drops by an amount $V \approx 14$ V. Then, however, the charge on these two electrodes (whose stray capacitance will be denoted by C_p) also changes, a negative charge $Q = C_p V$ being added to it. This charge is produced as follows.

Having been transferred one step to the left by a positive voltage step of the left-hand deflector plate, the beam tries to return to its former position, that is, to move to the right, during the trailing edge of the count-pulse. As will be seen from fig. 3, the anode current then tends to increase, thus providing extra current to charge the stray capacitance. The anode current increases all the faster, and the stray capacitance is therefore charged all the sooner,

the more rapidly the potential of the left-hand deflector plate is reduced.

The speed of these changes is limited owing to the fact that the above-mentioned extra current itself cannot exceed a certain limit. Some of the peaks of the $i_{a2} = f(V_{D',a_2})$ characteristic (see fig. 3) lie only about 100 μA above the stable points, and in fact, to ensure a thoroughly reliable result, we do not employ more than 20 μA of this margin (controlled by giving a suitable slope to the trailing edge of the count-pulse). The extra current (I) must reduce the potential difference across the stray capacitance (15 pF) by 14 V. The time required for this reduction is:

$$\vartheta_2 = \frac{C_p V}{I} = \frac{15\times10^{-12}\times 14}{20\times10^{-6}} \cdot 10^6 = 10.5 \ \mu\text{sec.} \quad (6)$$

If the build-up time (ϑ_1) of the pulse, and a certain safety margin, be added to ϑ_2, the duration of the pulse will be at least 13 μsec. Accordingly, ϑ_2 must be shortened. To see how this may be accomplished, let us consider equation (6). It will be clear that it is impossible to reduce either the stray capacitance C_p, or the potential difference V between two stable points. This leaves only the possibility of increasing the charging current I. It cannot be increased through the agency of the scaler tube itself; however, an extra current can be supplied from an outside source. Now, the direction of this current must be such that it produces a drop in the potential of the anode a_2 and the right-hand deflector plate D'; in other words, the current must supply electrons to these two electrodes. A current in the required direction can be obtained by connecting the anode of a suitable valve, e.g. a triode, to the right-hand deflector plate and the anode of the scaler tube (*fig. 6*). Such a "charging valve" must be cut off during the major part of the time, that is, it must pass current only for a brief period during the counting of a pulse.

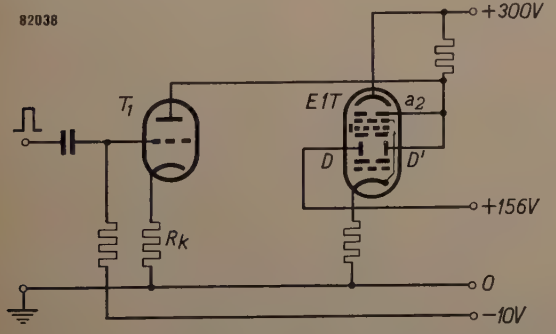

Fig. 6. Circuit to reduce the step-time by means of an auxiliary triode (T_1, "charging valve") which becomes momentarily conductive when gated by an incoming pulse and then supplies a negative charge to the right-hand deflector plate (D') of the scaler tube. The potential of the left-hand deflector plate (D) is constant (156 V). R_k cathode resistor.

Here, a difficulty arises, namely that the charging pulses applied must not be of uniform size, but should be smaller, the lower the voltage v_{D',a_2} of the right-hand deflector plate and the anode. Given a decrease in v_{D',a_2} (owing to the increase in anode current resulting from each step of the beam, i.e. 0-1, 1-2, and so on), the average potential in the space between the deflector plates will also decrease, by reason of the fact that the deflection is asymmetrical; hence the deflection-sensitivity will increase, that is, the stable points of intersection of the resistance line and the $i_{a_2} = f(v_{D',a_2})$ characteristic will lie closer together at a low, than at a high v_{D',a_2}. Now, the points *0,1, 2, ... 9*, as shown in fig. 3 are evenly spaced, but in fact the horizontal distance between *0* and *1* corresponds to 17.5 V (v_{D',a_2} being 245 V for position 0) and that between *8* and *9* to 12.8 V (v_{D',a_2} being 109 V for position 9)

Hence the ratio of the two extreme positions of the beam is $17.5 : 12.8 \approx 4 : 3$.

Accordingly, the circuit should be so designed that the charge supplied by the charging valve decreases with the anode voltage in such a way that the ratio of the charges consistent with the highest and lowest values of the anode voltage is 4 : 3. This condition is satisfied by providing the triode employed as a charging valve (fig. 6) with a suitable cathode resistor R_k, whose value can be established by the method illustrated in *fig. 7*. This diagram shows two characteristics of the triode

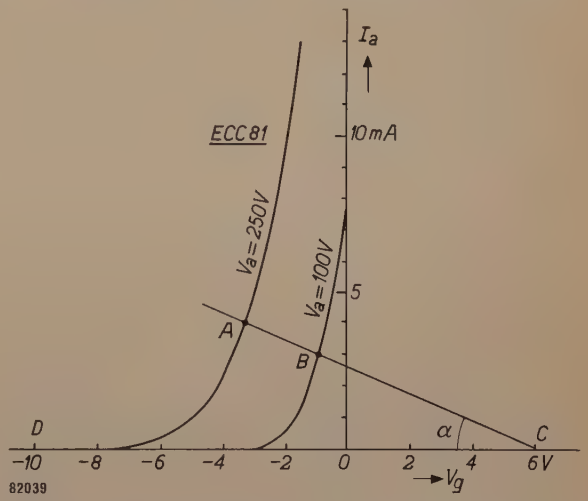

Fig. 7. $I_a = f(V_g)$ characteristics for $V_a = 100$ V and $V_a = 250$ V of one half of double triode ECC 81. Note the straight line drawn through points A (at 4 mA on the characteristic for $V_a = 250$ V) and B (at 3 mA on the characteristic for $V_a = 100$ V). It will be seen that this line makes an angle α with the V_g axis and cuts it at a point C. R_k (fig. 6) is equal to cot α. The required pulse amplitude is $CD = 16$ V.

employed (one half of a double triode ECC 81), viz. the anode current I_a plotted as a function of the grid voltage V_g for two values of the anode voltage V_a (100 V and 250 V). Now, a certain point A, corresponding to a current I_a defined by $I_a = Q/\Delta t = CV/\Delta t$ (where Δt is the duration of the pulse and V is 17.5 V), say $I_a = 4$ mA, is chosen on the characteristic for $V_a = 250$ V (practically equal to the highest anode voltage, 245 V), and another point B, whose ordinate is $^3/_4$ $I_a = 3$ mA, on the characteristic for $V_a = 100$ V (almost the lowest anode voltage, 109 V). The angle α of line AB then governs the size of R_k (= cot α). Line AB cuts the V_g co-ordinate at a point C, corresponding to $V_a = 6$ V. Since V_g must be about −10V to drive the valve far enough beyond cut-off at $V_a = 250$ V, the amplitude (DC) of the pulse must be about 16 V.

It is also necessary to establish the time Δt, since the precise value of R_k depends on it. Again, it is advisable to employ a pulse shaper capable of converting variable pulses (as produced, say, by a scintillation counter) into pulses of suitable size and constant duration required for counting. A suitable shaper is described in the Appendix (the pulse shaper shown in fig. 4 cannot be used here, since it does not produce pulses of the correct shape and duration.).

A charging current of 3 mA, that is, 150 times the original current (20 μA), is readily obtained by the above method. On the other hand, the charging valve almost doubles the stray capacitance of the scaler; despite this, however, an overall improvement by a factor of 75 is obtained, and time ϑ_2 is thus shortened to $10.5/75 = 0.14$ μsec.

The average dead-time τ_m may be calculated with the aid of formula (3), assuming firstly that the counts 0-1, 1-2, etc. involve no dead-time other than the 0.14 μsec already derived (hence $\tau_s = 0.14$ μsec), and secondly that the re-set time τ_r is still 27 μsec; we then have:

$$\tau_m = 0.9 \times 0.14 + 0.1 \times 27 = 0.13 + 2.70 = 2.83 \text{ μsec.}$$

Here, then, it would be possible to count, on the average, $10^{-3}/(2.83 \times 10^{-6}) = 3540$ random pulses per second (at 1 % loss).

In general, however, the apparatus preceding the scaler tube (scintillation counter, photomultiplier, amplifier, limiter, pulse shaper) is also affected by a certain dead-time (τ_c), usually exceeding 0.1 μsec, and in many cases even longer than 0.5 μsec. It will be evident that to make the dead-time of the scaler shorter than τ_c would serve virtually no useful purpose, since the scaler would then be ready to count some time before the preceding circuit could be ready to supply pulses.

In fact, we are really concerned only with the overall dead-time of the apparatus. This, also, can be calculated with the aid of equation (3), provided that τ_c be substituted for τ_s if it happens to exceed this, and likewise for τ_r if it be the greater of the two. Given $\tau_s = 0.14$ μsec, $\tau_r = 27$ μsec and $\tau_c = 1$ μsec, then, we have:

$$\tau_m = 0.9\,\tau_c + 0.1\,\tau_r = 0.90 + 2.70 = 3.60 \text{ μsec,}$$

which corresponds to: $n = 2800$ pulses/sec (at 1% loss).

Reducing the reset time

According to our original argument, the reset time is less important than the step-time as a means of increasing the counting rate for pulses occurring at irregular intervals. However, it will be seen from the last numerical example that the measures described so far enable the step-time to be so shortened that the major part of the average dead-time τ_m is in fact now the reset time τ_r. Although this in itself is reason enough to examine the possibility of reducing τ_r, there is a further reason, that is, that τ_r (and it alone) governs the maximum counting rate for periodic pulses.

Acceleration of the reset by means of a flip-flop circuit

The obvious course is to try to shorten the reset time in very much the same way as the step-time, that is, by employing an ancillary valve to reduce the retarding effect of the stray capacitance either by supplying, or by taking away, a charge.

During the reset, the potential of the right-hand deflector plate rises. To accelerate this rise — and so the reset — therefore, it is necessary to take away electrons from the right-hand deflector plate. Here, then, the cathode, not the anode, of the ancillary valve must be connected to the right-hand deflector plate (and the anode) of the counter tube.

Fig. 8 shows, in principle, how this may be done;

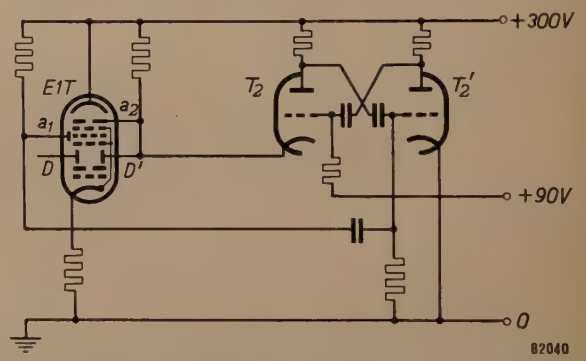

Fig. 8. Diagram showing scaler tube E1T with flip-flop circuit (T_2-T_2') to shorten the reset time. In the steady state T_2 is cut off and T_2' conductive. This negative pulse produced on the reset anode (a_1) when the beam returns from 9 to 0 reverses this situation.

a flip-flop circuit is employed. Ordinarily, the right-hand half T_2' of the valve in this circuit is conductive and the left-hand half (T_2) is cut off. However, a slight increase in the negative grid bias of T_2' is enough to reverse the situation; T_2' is then driven beyond cut-off and T_2 becomes conductive, thus drawing electrons from the right-hand deflector plate (D'), whose potential therefore rises very rapidly. This goes on until the current of T_2 decreases owing to the decrease in the potential difference between anode and cathode; T_2' then rises above cut-off and the circuit is restored to its original condition.

The flip-flop is triggered by the reset anode (a_1) of the scaler tube, that is, by a drop in the potential of this anode produced by the beam striking it each tenth pulse.

Circuits based on this principle lead to a very short reset time, viz. 4 μsec (ordinarily 27 μsec). Reduction of this time still further would involve the disadvantage that the auxiliary valve, whose anode current is inversely proportional to the reset time, would then draw a rather heavy current. Furthermore, these circuits impose a severe strain on the insulation between cathode and heater.

These disadvantages will now be explained. Consider the anode current first; during the reset, the cathode potential of the auxiliary valve T_2 rises from + 90 to about 245 V. To keep the valve about cut-off despite this rise, the potential difference between grid and cathode must remain virtually constant; in other words, the circuit parameters must be so chosen that the grid potential will also increase by about 245 — 90 = 155 V during the reset.

Unless the anode resistance be low, however, stray capacitance will make this increase too slow, and to obtain the necessary voltage drop across a low anode resistance it is necessary to employ a rather heavy current.

With regard to the heater insulation, if the heater be supplied from a transformer winding earthed, as usual, at the centre, the voltage between cathode and heater will rise well above the limit imposed on most valves. Hence it is necessary to employ a separate heater-current winding and to maintain it at a potential relative to earth roughly midway between 90 and 245 Volts (e.g. at 156 V, this being required, in any case, as bias for the left-hand deflector plate).

Despite this separate winding, however, even a very small leakage current may affect the count, since it will augment the anode current of the scaler tube and may thus eliminate one or more of the stable beam-positions. Accordingly, the auxilliary valve employed must have very good cathode-heater insulation.

However, in the circuit that will now be described, these disadvantages are avoided by employing a cathode with secondary, instead of thermionic, emission.

Acceleration of the reset by means of a secondary emission tube

Fig. 9 is the schematic representation of a secondary emission tube, type EFP 60. In this tube, primary electrons produced by a thermionic cathode (k_1) pass three grids (g_1, g_2 and g_3) and then strike the dynode (k_2). The dynode is an electrode coated with a substance with a high secondary emission factor, that is, a substance from which each incident primary electron releases several secondary electrons. Since the anode (a) is positive with respect to the dynode, the secondary electrons thus released proceed to the anode. By virtue of this secondary emission, the anode current of the tube exceeds its cathode current, the difference being supplied by the dynode.

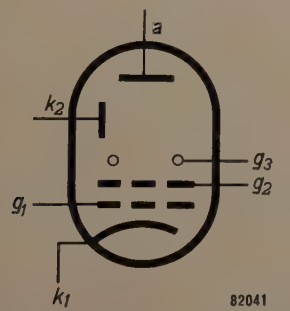

Fig. 9. Schematic representation of a secondary emission tube. k_1 thermionic cathode, g_1 control grid, g_2 screen grid, g_3 suppressor grid, k_2 dynode (secondary emission cathode), a anode.

Now, if the dynode be connected to the anode and to the right-hand deflector plate of the scaler tube (*fig. 10*), and the secondary emission tube be gated

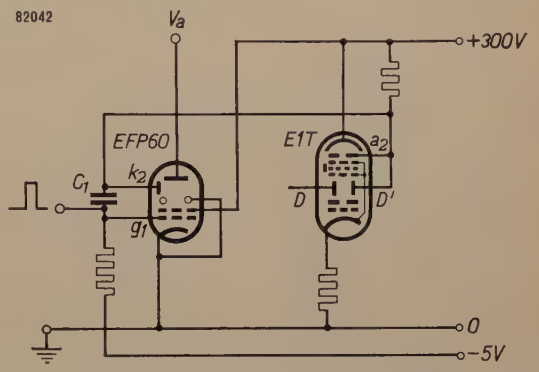

Fig. 10. Diagram showing scaler tube E1T with secondary emission tube EFP 60 to shorten the reset time. Tube EFP 60 is triggered by a positive pulse on g_1 and maintained conductive for the required period by coupling capacitor C_1 between k_2 and g_1.

at the correct moment, the desired effect will be obtained, that is, the dynode will draw electrons from the right-hand deflector plate, producing a sharp rise in the potential of this plate and thus accelerating the reset.

Here, then, we are presented with the problem of triggering the secondary emission tube at the correct moment.

To accomplish this, it is necessary to procure a positive voltage step on the control grid (g_1) at the precise moment when the reset is to take place. However, the only voltage step available at that moment is a negative one (on the reset anode, a_1, of the scaler tube). We therefore convert this negative step into the required positive one by means of a single stage amplifier between the reset anode and the control grid g_1 (*fig. 11*). In the present circuit, a double triode ECC 81 is employed, the one half (T_1') operating as an amplifier, and the other (T_1) as a charging valve to reduce the step-time (see fig. 6).

The secondary emission tube must remain conducting long enough to ensure the complete reset of the scaler tube. To ensure that it will do so, the control grid of the former is coupled to the dynode across a capacitor (C_1, fig. 10 and fig. 11); during the reset the potential of the dynode, and therefore

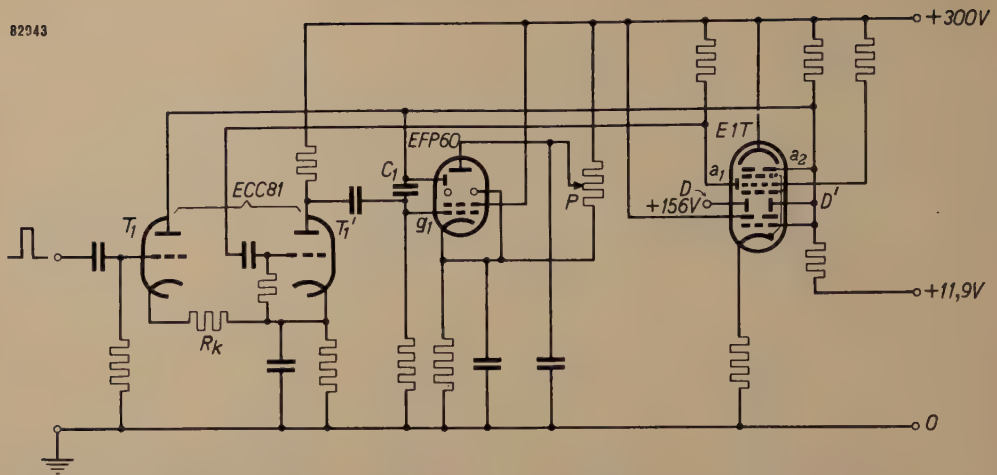

Fig. 11. Combination of the circuit shown in fig. 10, with that shown in fig. 6. The negative step produced on a_1 at the start of the reset is converted by amplifier T_1' into a positive step to bias the control grid (g_1) of secondary emission valve EFP 60. P potentiometer to control the anode voltage of valve EFP 60 (that is, to compensate for variations between individual scaler tubes). T_1 is a charging valve to shorten the step-time (see fig. 6). T_1 and T_1' are the two sections of a double triode ECC 81.

that of the control grid, rises, thus maintaining the valve in operation.

The dynode potential continues to rise until it nearly equals the anode potential; then, however, secondary electrons return to the dynode, the rise in the potential of this electrode reaches its limit, and the beam reaches the end of the reset. Here, then, we have a simple means of compensating for variations as between individual E1T scaler tubes, that is, for differences in the particular voltage V_{D',a_2} associated with position 0; without such compensation, the beams in some of these tubes might well reset only as far as position 1, instead of to position 0, owing to the above-mentioned "spread". The method of compensation consists in making the anode voltage of the secondary emission valve variable (potentiometer P in fig. 11).

After the reset, the positive charge leaks away from the control grid of the secondary emission tube, thus cutting off the tube and restoring the original situation.

The circuit shown in fig. 11 enables the reset time to be reduced to 0.45 μsec, thus raising the maximum counting rate for *regular* pulses to 2.2 million per second (*fig. 12*).

As far as *random* pulses are concerned, it should

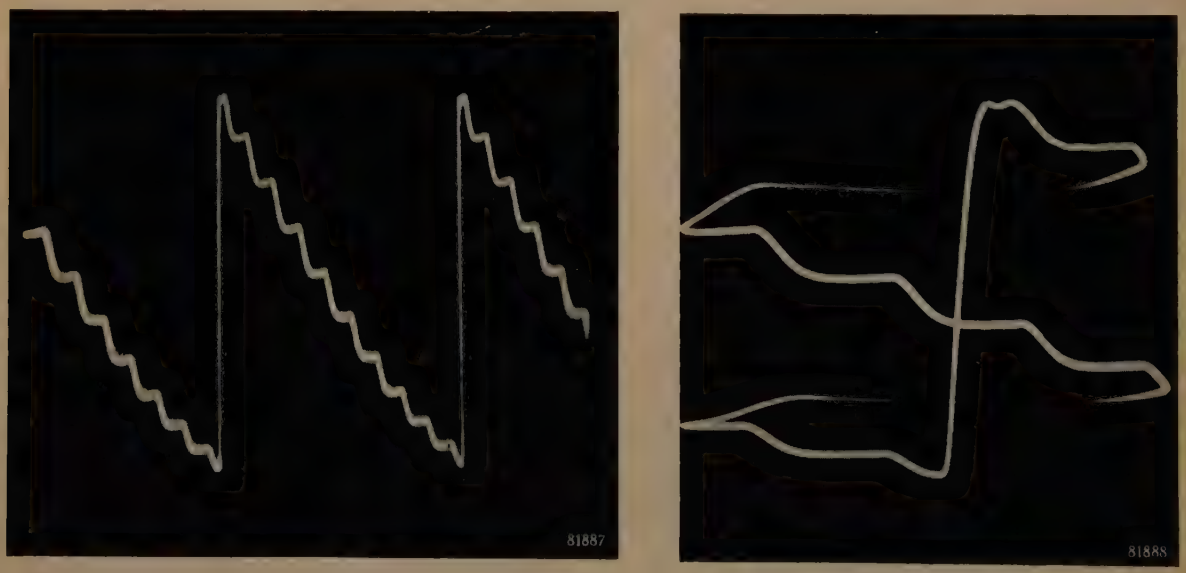

a *b*

Fig. 12. Oscillograms of V_{D',a_2} in the circuit shown in fig. 11, taken during a count of regular pulses at the rate of 2 million per second; the peak count rate attained by the scaler was 2.2 million. Note that the speed of horizontal deflection was made a factor of four greater in (*b*) than in (*a*); this was done for more accurate measurement, particularly of the reset time.

be borne in mind that a scintillation counter with a photomultiplier has a dead-time of about 0.20 μsec (see the articles referred to in note [2])). This exceeds the step-time of 0.14 μsec obtained in the manner described; at the same time, the contribution of the reset to the average dead-time is only $0.1 \times 0.45 = 0.045$ μsec. The average dead-time is therefore:

$$\tau_m = 0.9 \times 0.20 + 0.045 = 0.225 \text{ μsec.}$$

Accepting a loss of 1%, this value of τ_m corresponds to a counting rate for random pulses of 44 500 per second; this rate increases directly proportionally to the loss which is acceptable.

Finally, it should be noted that in as far as this article refers to laboratory work, the results quoted in this article take no account of tolerances on valves and other circuit elements, whereas such tolerances are included in the results given in article I.

Appendix: A pulse shaper to drive the charging triode

To operate efficiently, the charging triode, which shortens the step-time (T_1 in fig. 6 and fig. 11), should be driven by pulses of constant height and width. However, the pulses produced by particle counters, particularly scintillation counters, do not satisfy this requirement. Hence a pulse shaper is employed to convert them into pulses of uniform width and of the required amplitude. To give an idea of the manner in which such a pulse shaper operates, one or two of the possible designs will now be briefly described.

Every elementary particle striking the particle counter ultimately produces an avalanche of electrons, that is, in the tube itself if it be a Geiger-Müller tube, and in the associated photomultiplier if a scintillation counter is employed. The electrons so produced strike an electrode, thus charging its stray capacitance which subsequently discharges through a resistor (*fig. 13*). In this way, saw-tooth voltage pulses having a

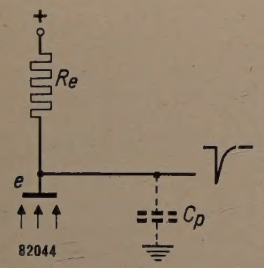

Fig. 13. Each elementary particle striking a particle counter produces an avalanche of electrons on electrode. *e* This, in turn, produces at this electrode a negative voltage step having a steep front and an exponential decay. The time constant of this tail is R_eC_p, where R_e is the charging resistance of electrode *e* and C_p the stray capacitance.

steep front and an exponential decay are produced. Owing to the appreciable variation between the individual charges supplied, the pulses differ considerably in amplitude, the amplitude variation between suitable pulses being as 1 : 20; the smallest pulses are those which just emerge above the noise-level. Since the time constant of the exponential decay is the same for all the pulses, the differences in amplitude correspond to differences in duration.

The usual procedure is to cut down the peak pulses to some extent by limiting, the signal thus obtained being employed — if necessary after amplification — to control a multivibrator, e.g. as shown in *fig. 14*. The multivibrator reverses every time the input signal passes a certain level. The output signal then consists of square-waves equal in amplitude but different in duration. Now, pulses of uniform duration can be obtained by differentiating the square-wave signal in an *RC* network; this produces identical positive and negative pulses. If desired, the negative pulses can be cut off by means of a diode.

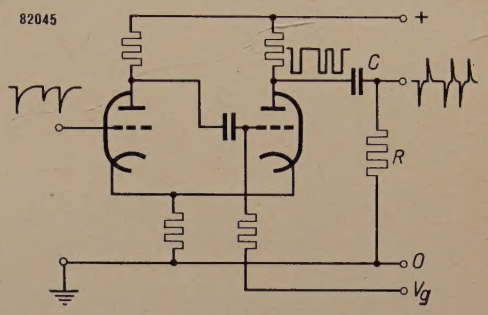

Fig. 14. Diagram of a multivibrator to convert incoming, dissimilar pulses into square pulses of uniform amplitude but different widths. Positive and negative pulses identical in shape and size are obtained by differentiating these square pulses (capacitor *C*, resistor *R*). The input-voltage level to trigger the multivibrator can be varied by varying the grid bias V_g.

The input-signal level to trigger the multivibrator can be varied by varying the grid bias V_g (fig. 14), this bias then being so adjusted that the smallest pulses that can be regarded as noise, have no effect. However, this involves the disadvantage that two pulses arriving in quick succession are likely to be counted as one, since if the second pulse happens to arrive before the first has dropped below trigger level (*fig. 15*), it cannot trigger the multivibrator and will therefore be missed in the count.

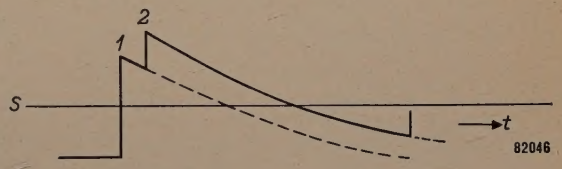

Fig. 15. If the second of two successive pulses (*2*) arrives before the first (*1*) has dropped below the trigger-level (*S*) of the multivibrator (fig. 14), pulse *2* will not be counted.

A considerable improvement in this respect is obtained by employing a delay line in the pulse shaper (*fig. 16a*). The electron avalanche on electrode *e* produces a negative voltage step at *e*. This step is propagated along the line (that is, from right to left in the diagram). Now, the end of the line is short-circuited, so that reflection with change of sign takes place, producing a positive step which travels from left to right. The input end of the line is terminated with a resistor (viz. resistor R_e, through which electrode *e* is supplied): this resistor matches the characteristic impedance of the line and therefore prevents reflection at the input. The effect of this arrangement is, then, that the negative step is followed, after an interval equal to twice the delay-time of the line, by a positive step, the two steps finally combining to form one square pulse (fig. 16*b*). All that is then necessary to make such a square pulse suitable to drive the charging triode is to change its sign and give it the required height.

Since a real transmission line providing the necessary delay would be many metres long, an artificial transmission line is employed; this may be a filter of coils and capacitors, or a specially designed transmission line, of high self-inductance and capacitance per unit length so that the required length is kept within reasonable bounds (say 10 or 20 cm).

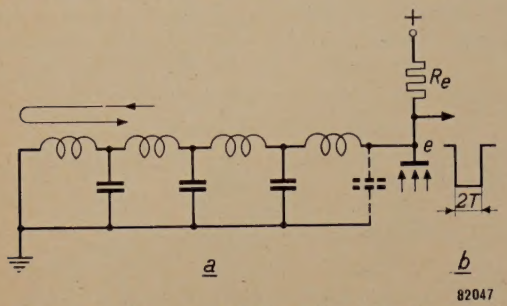

Fig. 16. Diagram showing (*a*) that if a delay line of characteristic impedance R_e, short-circuited at the free end, be connected to anode *e* (fig. 13), the electron avalanche will produce on this anode square pulses (*b*), whose duration is twice the delay (T) in the line.

In practice, it may be necessary to employ one decade scaler in conjuction with several particle counters whose pulse shapers produce pulses differing in width. Here, it would be necessary to vary the bias resistance R_k of the charging triode for each incoming pulse, which would not only be difficult in itself, but would also be a possible source of error in the count; thence it is better to introduce another pulse shaper (*C*, *fig. 17*) to convert the different pulses into identical

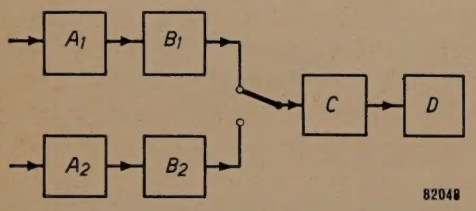

Fig. 17. A_1, A_2 particle counters, and B_1, B_2 their associated pulse shapers. If the pulses produced by B_1 and B_2 differ in duration, another pulse shaper (*C*) should be added to convert these pulses into pulses of uniform duration. *D* scaler.

ones. By a fortunate chance, the charging triode is able to operate with pulses shorter than those produced by most particle counters. When once the dissimilar pulses have been rendered uniform in amplitude by a limiter, pulses of identical (triangular) shape can be derived from them (*fig. 18*); these derived pulses are very short, but nevertheless usable. If the amplitude of such triangular pulses is too small, they can be re-converted into square pulses by means of a multivibrator. Any sensitivity on the part of the counter to the width of the original pulses is thus eliminated.

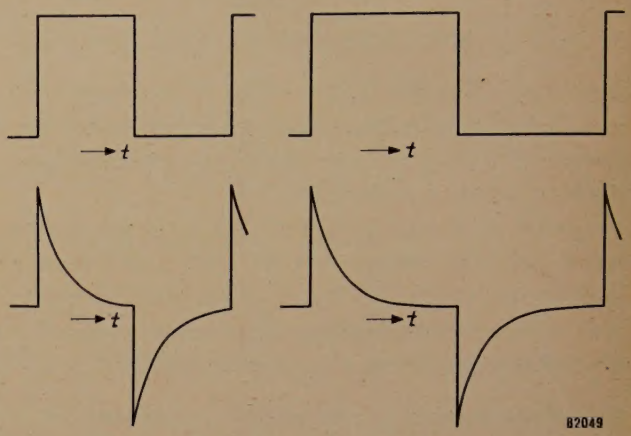

Fig. 18. The identical triangular pulses to gate the charging triode (T_1 in fig. 6 and fig. 11) are obtained by differentiating square pulses uniform in amplitude but differing in width.

Summary. This article describes circuits developed to count as many pulses per second as possible, particularly random pulses by means of a decade scaler tube type E1T. Tube E1T has two "dead-times", viz. the step-time (τ_s) required for each step (0-1, 1-2,..., 8-9), and the re-et time (τ_r) to return the beam from 9 to 0. The maximum counting rate for regular pulses is governed entirely by τ_r (since $\tau_r > \tau_s$). In the case of random pulses, an "average dead-time" (τ_m), depending on τ_s as well as τ_r, governs the counting rate; here, the average number of pulses recorded per second (n) is invariably smaller than the number of pulses arriving per second (N). Provided that N is not taken unduly large, the difference between it and n will be negligible, e.g. less than 1%. Where N is relatively large, its value can be calculated from n with the help of a correction factor. The effect of a possible inaccuracy in τ_m is more apparent in the correcting factor, the greater the difference between N and n.

An improved pulse shaper, a method of shortening the step-time, and two methods of shortening the reset time are described. The highest count rates attained are 44 500 random pulses per second with a loss of 1%, and 2.2 million regular pulses per second. Particulars of the pulse shaper used in the circuit for shortening the step-time are given in an appendix.

ABSTRACTS OF RECENT SCIENTIFIC PUBLICATIONS OF N.V. PHILIPS' GLOEILAMPENFABRIEKEN

Reprints of these papers not marked with an asterisk * can be obtained free of charge upon application to Philips Electrical Ltd., Century House, Shaftesbury Avenue, London W.C. 2.

2150: K. ter Haar and J. Bazen: The titration of bismuth with "Complexone III" at *p*H 2.0-2.8 (Anal. chim. Acta **10**, 108-112, 1954, No. 2).

A titration procedure for Bi is described; by adding an excess of "Complexone III" (Versene) and back-titrating at *p*H 2.0-2.8 with standard thorium nitrate solution using "Alizarin-S" as an indicator, it is possible to determine Bi with a precision of about 0.3%.

By choice of the proper *p*H it is possible to eliminate most of the interfering elements, but at *p*H 2.0, Fe and Ni and Cu (slightly) still interfere. Attention is drawn to the fact that it may be possible to determine Bi at *p*H 2.0 by direct titration with "Complexone III" in the presence of excess tartrate, using thiourea as an indicator. This method might be of value in the presence of Sn and Sb.

2151: E. W. Gorter: Ionic distribution deduced from the g-factor of a ferrimagnetic spinel: Ti^{4+} in fourfold coordination (Nature, London **173**, 123, 1954, Jan. 16).

Where, in oxides with spinel structure, the distribution of metallic ions over tetrahedal (*A*) and octahedral (*B*) sites cannot be found with sufficient accuracy by X-ray diffraction, magnetic data may provide the necessary information, particularly the saturation moment and the factor $g = 2M_{tot}/M_{spin}$, where M_{tot} is the magnetic moment due to orbits plus spins. Because of the negative exchange coupling, the *M*'s are equal to the difference $M_A - M_B$ for both kinds of ions. It is found that for a ferrite $Ni^{2+}_{1.5}\ Fe^{3+}\ Ti^{4+}_{0.5}\ O^{2-}_4$, the distribution corresponds to the formula $[Fe_{0.7}\ Ti_{0.3}]_A\ [Ni_{1.5}\ Fe_{0.3}Ti_{0.2}]_B\ O_4$.

2152: L. Heijne, P. Schagen and H. Bruining: Television pick-up tube for both light and X-ray pictures (Nature, London **173**, 220, 1954, Jan. 30).

Short description of a television camera tube provided with a screen consisting of lead oxide, evaporated on a "Pyrex" glass window. The layer is scanned by a low-velocity electron beam. The light sensitivity (peak in blue part of spectrum) amounts to 100-200 μA/lm ($T_C = 2600$ °K). The relatively high sensitivity to X-rays is the result of the high absorption coefficient of lead (5% absorption in a 5 micron layer for 70 kV D.C; filter 5 mm Al). Photographs are given, showing the same objects illuminated with visible light and with X-rays (shadow picture.)

2153: R. van der Veen and J. Daams: Experiments on the growth of helianthus seedlings (Proc. Kon. Ned. Akad. Wetensch. Amsterdam, Serie C**57**, 81-91, 1954, No. 1).

The growth of isolated parts of the stems of helianthus seedlings in light and in darkness was investigated. The experiments indicate that the growth of green stem sections is controlled by a photochemical reaction. This reaction results in a much quicker generation of organic phosphates, which in turn accelerates growth if auxin is present. The formation of phosphates is not due to enhancement of respiration by illumination, as is evident from the fact that stem parts containing no chlorophyll showed no enhanced respirations. Therefore photosynthesis is more probable. This is corroborated by an investigation on spectral sensitivity to be dealt with in a forthcoming paper.

2154: A. Claassen, L. Bastings and J. Visser: A highly sensitive procedure for the spectrophotometric determination of aluminium with 8-hydroxyquinoline and its application to the determination of aluminium in iron and steel (Anal. chim. Acta **10**, 373-385, 1954, No. 14).

Aluminium hydroxyquinolate can be quantitatively extracted by chloroform from an ammoniacal solution containing hydroxyquinoline, complexone and cyanide.

Titanium, vanadium, tantalum, niobium, uranium, zirconium, gallium, antimony, bismuth, indium and traces of beryllium are similarly extracted. Aluminium can be separated from the first five elements by an extraction in ammonical solution containing hydrogen peroxide. Zirconium, gallium, bismuth and antimony can be eliminated by a cupferron extraction and indium by extraction with diethyldithiocarbamate. Beryllium is eliminated by performing an extraction with hydroxyquinoline at *p*H 5. The proposed method enables a practically specific photometrical determination of aluminium. Applications are given of the determination of trace and

higher amounts of aluminium in steels, non-ferrous alloys and in glass.

2155: W. J. Oosterkamp: General consideration regarding the dosimetry of roentgen and gamma radiation. Addendum. (Appl. sci. Res. **B3**, 477-478, 1954).

Addition to the original paper under the same heading (Appl. sci. Res. **B3**, 100-118, 1953) to adapt this to the new recommendations of the International Commission on Radiological Units (Copenhagen, July 1953). The definitions of the new quantity *absorbed dose* and the unit in which this quantity is measured, the rad (= 100 erg/gram) are given.

2156: H. P. J. Wijn: Ferromagnetische resonantie en relaxatieverschijnselen (Ned. T. Natuurk. **20**, 45-53, 1954, No. 3). (Ferromagnetic resonance and relaxation phenomena; in Dutch.)

See these abstracts, No. **2092** and **2128**.

2157: J. Volger: Further experimental investigations on some ferromagnetic oxidic compounds of manganese with perovskite structure (Physics **20**, 49-66, 1954, No. 1).

Polycrystalline substances of the type $La_{1-\delta}Sr_{\delta}MnO_3$ have been investigated. These are ferromagnetic semiconductors which exhibit some remarkable second order effects related to the electrical conductivity. The specific heat has been found to be in agreement with Weiss' theory. New data on the direct current resistivity including that at liquid hydrogen temperature have been obtained. The direct current magneto-resistance appears to be independent of the mutual orientation of magnetic field and current; most of the effect seems to be due to domain rotations. The alternating current resistivity of some samples depends strongly upon frequency and high values of the dielectric constant have been observed at low frequencies. Samples exhibiting these properties also show a magneto-resistance dependent on the frequency of the alternating current, and a variation of both resistivity and magneto-resistance with applied voltage. These effects strongly support the hypothesis of barrier-layer resistance in ceramic semiconductors. A phenomenological analysis of these effects is given and may be of some importance for the general problem of magneto-resistance in ferromagnetics. The Seebeck effect of various samples is roughly in agreement with certain basic ideas on conductivity in oxidic semiconductors. From Hall effect measurements no conclusions could be drawn except that the apparent electron mobility is extremely small.

2158: E. J. W. Verwey: Oxyd-Systeme mit interessanten elektrischen und magnetischen Eigenschaften (Angew. Chemie **66**, 189-192, 1954, No. 7). (Oxidic systems with interesting electric and magnetic properties: in German.

Survey of properties of oxidic compound systems containing elements of the first transition period of the periodic system. Sintered ceramic materials with the NaCl, haematite and spinel lattice are described, which are of interest as semiconductors for the production of resistance materials and further provide magnetic materials of industrial importance.

2159: F. A. Kröger and H. J. Vink: The origin of the fluorescence in self-activated ZnS, CdS, and ZnO (J. Chem. Phys. **22**, 250-252, 1954).

It is proposed that the luminescent centre in "self-activated" ZnS consists of a cation vacancy whose nearest surroundings have lost one electron. Such a centre is consistent with the fact that at low firing temperatures, the appearance of the blue fluorescence of self-activated ZnS depends upon the presence of "promoter ions" (monovalent anions or trivalent cations) whereas, if the firing temperature be sufficiently high, some blue fluorescence is obtained without the presence of such promoter ions. The luminescence of reduced ZnS, CdS, and ZnO is also discussed, and is attributed to anion vacancies that have trapped one electron.

2160: S. Duinker: Magnetische versterkers (T. Ned. Radiogenootsch. **19**, 91-114, 1954, No. 2). (Magnetic amplifiers; in Dutch.)

A simplified graphical analysis of the principle of operation of magnetic amplifiers, based on an idealized *B-H* characteristic of the core material, under no-load conditions. Two fundamental types, the series-connected and the parallel-connected magnetic amplifier are considered. The factors determining the power-amplification, feedback, supply frequency, core-construction and bias are discussed.

A survey is given of the properties of magnetic amplifiers and the applications in various fields, which can be broadly separated into measurement, control, switching and a.c. amplification.